BERICHTE AUS DEM MARUM UND DEM FACHBEREICH GEOWISSENSCHAFTEN
DER UNIVERSITÄT BREMEN

R/V HEINCKE
Cruise Report HE450

Dynamics of Gas Emissions along the Barents Sea Svalbard Margin

Tromsø – Tromsø
25 August – 08 September 2015

Bohrmann, G.
Ferreira, Chr., Hong, W.-L., Hsu, C.-W., Lange, M., Loher, M., Pape, T., Torres, M., Wintersteller, P., Yao, H.

Cruise sponsored by Deutsche Forschungsgemeinschaft (DFG) through
MARUM – Center for Marine Environmental Sciences

The cruise was performed by
MARUM – Center for Marine Environmental Sciences

2016

marum

Universität Bremen

R/V HEINCKE Cruise Report HE450

Table of Contents

1 Preface

Gas emissions from the continental margin and the shelf west of Spitsbergen became recently well known (e.g. Westbrook et al. 2009; Sahling et al. 2014). Specifically west of Prins Karls Forland gas emissions in around 400 m water depth have been interpreted from decomposing hydrates due to a temperature increase from 2°C to 3°C over the last 30 years (Westbrook et al. 2009). Although this interpretation is not accepted by all scientists the global impact of that mechanism would be very important in the context of global change. Investigations on that problem are therefore highly welcome. During R/V HEINCKE HE450 (Fig. 1) we explored gas emissions using the echosounders of the ship along the slope of the Barents Sea up to Svalbard to find more evidence for dynamic changes of gas hydrates and emissions of free gas.

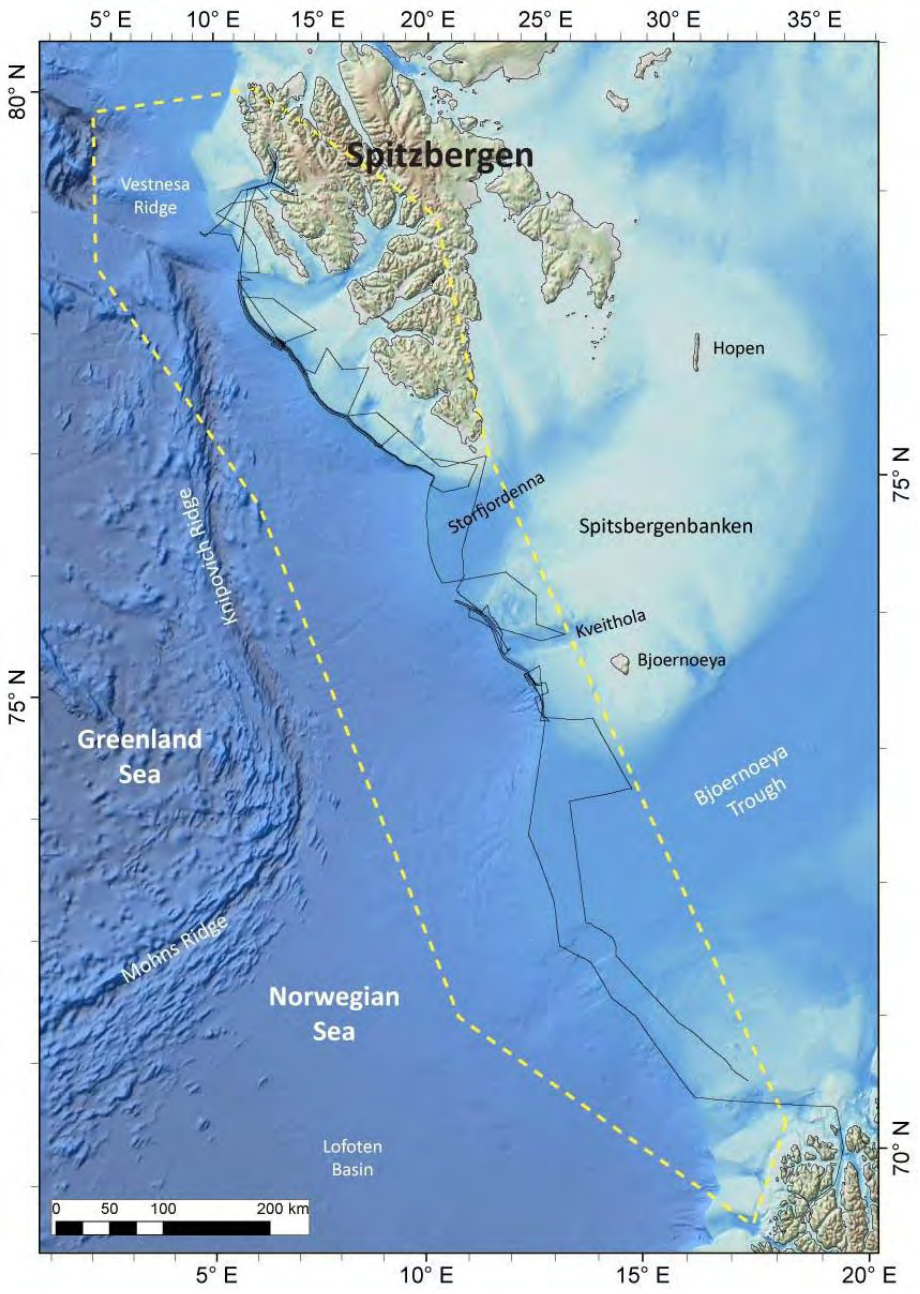

Fig. 1: Track lines of R/V HEINCKE Cruise HE450 along the northernmost European margin of the Nordic Seas. The outline of the area of permission is shown by the stippled line.

R/V HEINCKE Cruise HE450 was requested and planned within the BMWi project IMGAM „Intelligentes Monitoring von klimaschädlichen CO_2/CH_4 Gasaustritten im Meer“, to investigate gas emission sites at the seafloor of the western margin of Spitsbergen. The cruise was coordinated and carried out by MARUM Center for Marine Environmental Sciences at University of Bremen. The shipping operator Reederei Briese Schiffahrts GmbH & Co KG provided technical support on the vessel. We would like to especially acknowledge the Master of the vessel Werner Riederer, and his crew for their continued contribution to a pleasant and professional atmosphere aboard R/V HEINCKE. We thank the Federal Ministry of Economics for financial support of the cruise. We also thank our logistic department, specifically Götz Ruhland, and Marcon Klann, the MARUM administration department and Angelika Rinkel and Greta Ohling for their help in preparing the cruise and support during the postprocessing.

Fig. 2: Scientific crew onboard R/V HEINCKE HE450. The photo was taken in Ny Ålesund where R/V HEINCKE berthed for two hours, meanwhile the scientists visited the German Koldewey Station in this northernmost settlement of scientists.

Personel aboard R/V HEINCKE

Table 1: Scientific crew

Name	Discipline	Affiliation
Bohrmann, Gerhard	Chief scientist	MARUM
Ferreira, Christian	Multibeam	MARUM
Hong, Wei-Li	Pore water chemistry	CAGE
Hsu, Chieh-Wei	Mapping, sediments	GeoB
Lange, Mirko	Chemistry, ICOS	GeoB
Loher, Markus	Sediments, mapping	MARUM
Pape, Thomas	Gas analyses, Cores	MARUM
Torres, Marta	Pore water analyses	OSU
Wintersteller, Paul	Hydroacoustic, IT, mapping	MARUM
Yao, Haoyi	Geochemistry	CAGE

MARUM Center for Marine and Environmental Sciences, DFG Research Center and Cluster of Excellence, University of Bremen, Postfach 330440, 28334 Bremen, **Germany**

GeoB Department of Geosciences, University of Bremen, Klagenfurter Str., 28359 Bremen, **Germany**

OSU Oregon State University, Corvallis OR, **USA**

CAGE Centre for Arctic Gas Hydrate, environment and climate, Dramsveien 201, 9010 Tromsø, **Norway**

Werner Riederer | Remo Franke | Marvin v. Aswegen | Klaus-Dieter Klinder | Wolfgang Starke | Heiko Baron

Stefan Trautmann | Steffen De Vries | Bruno Vareio Do Amaral | Derk Heeren | Martin Dräger | Ronald Klafack

Fig. 3: Crew members onboard R/V HEINCKE HE450.

Table 2: Crew members onboard

Name	Discipline	Name	Discipline
Riederer, Werner	Master	Trautmann, Stefan	A.B.
Franke, Remo	Chief Mate	De Vries, Steffen	A.B.
von Aswegen, Marvin	2.NO	Vareiro Do Amaral, Bruno	A.B.
Klinder, Klaus-Dieter	Chief Engineer	Heeren, Derk	A.B.
Starke, Wolfgang	Electrician	Dräger, Martin	A.B.
Baron, Heiko	Boatswain	Klafack, Ronald	Cook

Shipping operator: Briese Schiffahrts GmbH & Co KG, Abteilung Forschungsschifffahrt, Hafenstr. 12, 26789 Leer, **Germany**

2 Introduction

(G. Bohrmann)

2.1 Geological Setting of Svalbard and Barents Sea Shelf

Svalbard forms an Arctic archipelago at the northwestern edge of the Barents shelf, far north of Norway. Svalbard is the official Norwegian name for the archipelago, which includes all islands between 74° and 81°N, and 10° and 35° E like Spitsbergen, Bjørnøya, Hopen and Kong Karls Land. Geologically Svalbard is the emergent northwestern corner of the Barents shelf, which was uplifted by Late Mesozoic and Cenozoic crustal movements. The record of rocks ranges in age from Precambrian to Recent and the geological history includes several tectonic events from Neoproterozoic to Early Palaeogene. Passive continental margins occur to the north to the Eurasian Basin and offshore to the west to the northern part of the Atlantic Ocean where the Knipovich Ridge is forming the plate boundary between the North American and the Eurasian Plates. The central part of the ridge, the active spreading zone is highly segmented by transform faults from which the Molly and Spitsbergen Fracture zones are the pronounced examples. When seafloor spreading started in the Nordic Seas in the Eocene about 52 Ma ago (Magnetic Anomaly 24), Svalbard and the Barents Shelf were tectonically separated from Greenland by a continental transform fault system from which the present Hornsund Fault complex was part of it (Dallmann 2015).

The Barents Sea Shelf between Svalbard and Fennoscandia is a platform area. Precambiran crust is mainly buried under thick pile of Late Palaeozoic to Neogene sedimentary rocks. The western margin includes an extension of the Ordovician-Silurian (Caledonian) Orogen. Structural basins and elevations of the sedimentary sequences were formed under the influence of transform faulting and crustal extension during the formation of the North Atlantic basin. Those basins like the Sørvestsnagsen, Trømsø or Hammerfest basins (Ostanin et al. 2013) contain oil and gas fields often with shallow gas deposits. Leakage of thermogenic methane was well shown in seismic records and seafloor expressions like pockmarks and acoustic flares (e.g. Ostanin et al. 2013; Chand et al. 2012).

The western margin of Spitsbergen is influenced by the landward continuation of the slow-spreading Knipovich Ridge. It is a segmented, sheared transform margin partly characterized by under-plating of thinned oceanic crust (Ritzmann et al., 2004) which may generate together with magmatic intrusions at the continent-ocean boundary a higher geothermal gradient (Vanneste et al. 2005). The area was repeatedly glaciated and accordingly experienced rapid changes in sea-level sedimentation and erosion (Landvik et al. 2005; Svendsen et al., 2004). The ice of the Svalbard-Barents Sea Ice Sheet of the last major glaciations on Svalbard retreated from this margin approximately 13 ka ago (Landvik et al., 2005). The present rate of uplift in Svalbard is 4-5 mm/yr (Sato et al., 2006) which is a combination of post-glacial rebound and acceleration from recent ice loss of retreating glaciers on Svalbard.

The western continental shelf off Svalbard is morphologically characterized by the glacial cross shelf troughs of Kongsfjord, Isfjord, Bellesund, Hornsund and Storfjord, their lateral and terminal morainal ridges and their broad trough mouth fans. The sedimentary architecture is composed of glacigenic debris flows of the trough mouth fans (TMF), hemipelagic glacio-marine sediments occasional forming drift bodies of contourite deposits and the transitional areas between them. The alternation of hemipelagic deposits with stacked debris flows have been identified to play an important role for preconditioning of submarine slides due to the increase of pore pressure in

sediments between less permeable layers under load (Winkelmann & Stein 2007). Fluid and gas migration on this shelf occurs along major geological structures (Knies et al. 2004). The occurrence of large areas with bottom-simulating seismic reflectors indicates the presence of gas hydrates and pockmarks (Vogt et al. 1994; Vanneste et al. 2005).

2.2 Gas Venting at the Western Svalbard Margin

The Arctic region is warming faster than other regions on our planet. Since the Arctic Ocean is also storing methane hydrates at its margins, significant amounts of methane can be released (Archer and Buffett, 2005). Hydrates are stable under low-temperature and high-pressure conditions. Methane hydrates in high-latitude regions are characterized by relatively low bottom-water temperatures and can therefore persist in relatively shallow water depths. Because those regions are highly sensitive to increase in bottom-water temperatures in the course of global warming, shallow hydrates are highly susceptible to thermal dissociation, which might lead to methane release from the seafloor. Moreover, methane escaping the seafloor at shallow depths eventually reaches the atmosphere, where it might contribute as greenhouse gas to further global warming (Mienert et al. 2010).

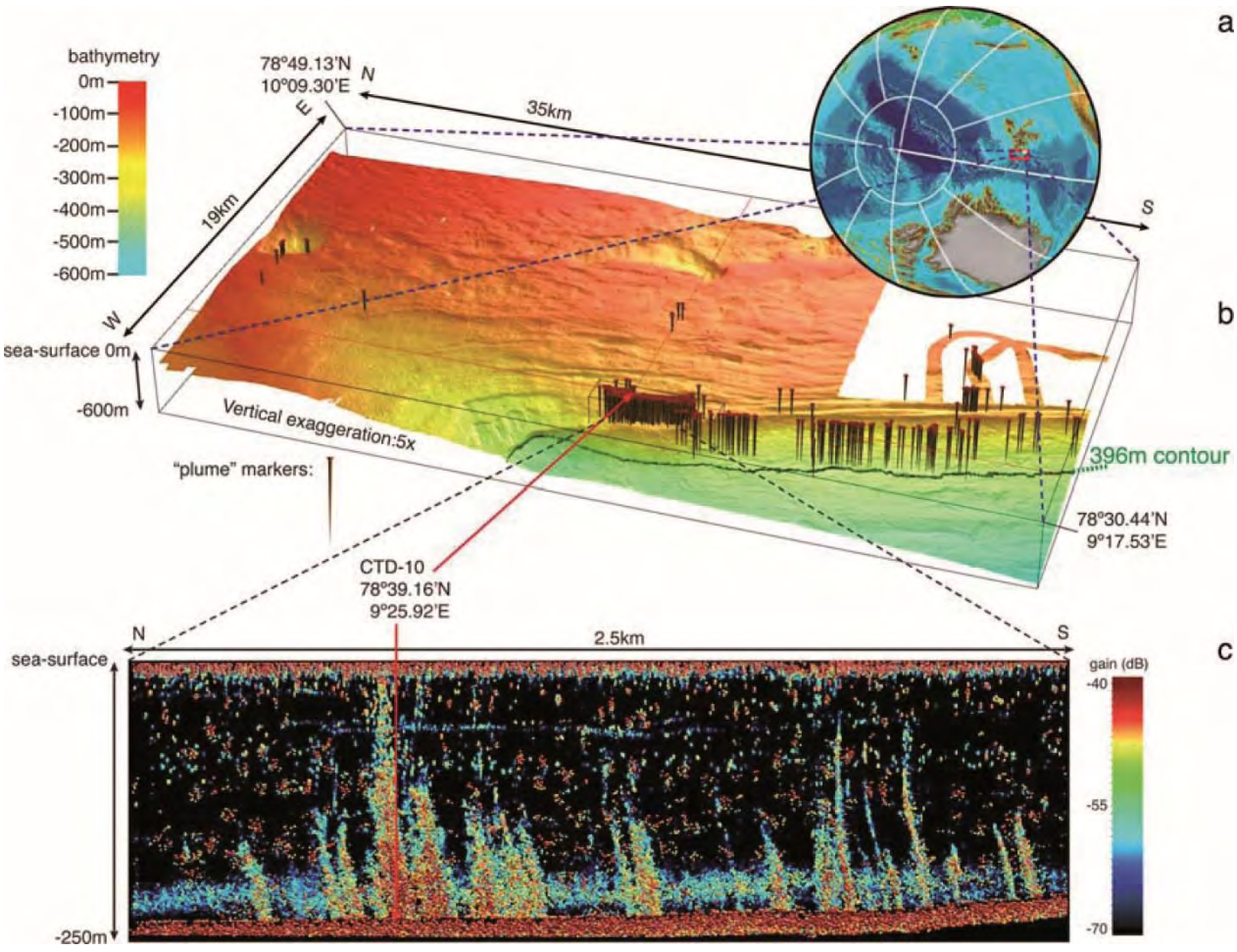

Fig. 4: Location of survey west of Svalbard (a), position of flares imaged by EK60 during JR211 superimposed on perspective view of bathymetry (b), part of the record from the acoustic survey showing examples of observed gas plumes (from Westbrook et al. 2009).

In this light, the finding of numerous gas emissions at the continental margin west of Svalbard (Fig. 4) concentrated along the 396 m isobaths representing the upper limit of the gas hydrate stability zone was alarming. Westbrook et al. (2009) argued that during the last three decades, the bottom water at that depth has increased from 2°C to 3°C assuming that the upper boundary of the GHSZ deepened from 360 m to 396 m. This temperature increase could have caused hydrate dissociation in the sediments and, as a consequence, bubbles of free gas are emitting to the water column (Fig. 5). If this interpretation is right, then this location would be the first site where the hypothesis of global warming-induced hydrate dissociation may actually be confirmed.

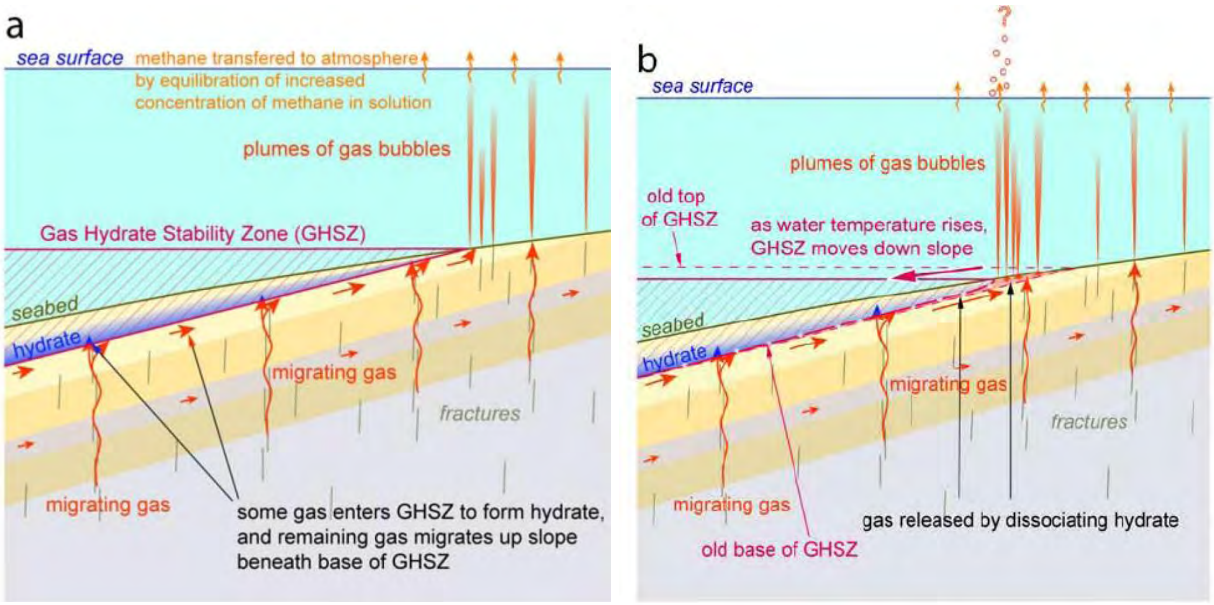

Fig. 5: Scenario described by Westbrook et al. (2009): (a) Migrating methane gas is restricted from reaching the seabed in the GHSZ by its conversion to hydrate and by the overall reduction in permeability caused by the growth of hydrate at the base of the GHSZ. Methane gas escaping from the seabed beyond the GHSZ rises as bubbles through the seawater. (b) An increase in the temperature of the seawater causes the GHSZ to contract down slope, dissociating hydrate to methane and water. Where the GHSZ is removed entirely, all the released gas is free to move to the seabed, guided by local variation in lithology and structure. Where a thinner GHSZ remains, gas from the dissociated hydrate at its base can migrate into the GHSZ to form hydrate again and may also migrate up slope.

However, Westbrook et al. (2009) offered also alternative hypothesis for the slope-parallel presence of seafloor gas emissions. Free methane in the deep slope sediments may migrate upward along the base of the GHSZ, because of the sealing effect of concentrated hydrate (Fig. 5). The free gas could escape the sediments where the GHSZ is outcropping and could therefore explain a clustering of the gas emissions at the depth around 396 m. Theories including gas hydrates to explain the clustering of emission sites around 396 m are not verifiable, because gas hydrates have not been documented by sampling or geophysical documentation so far. Sampling using conventional methods like gravity or piston coring from research vessels failed up to now because of the difficult lithology which did not allowed for cores to penetrate. Sampling this shallow sediment sequence by drilling using a mobile drilling system (Freudenthal and Wefer, 2013) will probably happen in August 2016 and is even not available by now. The presence of hydrate is documented by a clear bottom-simulating seismic reflector (BSR) at this continental margin below 600 m water depth (Vanneste et al., 2005; Chabert et al., 2011). In addition, hydrates were recovered from shallow sediments in around 900 m water depth (Fisher et al., 2011).

Further investigations at the gas emission sites were performed by Berndt et al. (2014). Uranium–thorium dating of methane-derived authigenic carbonates sampled at the seafloor of the gas emission sites revealed ages of up to 3000 years for the carbonate formation. Since carbonate precipitation is related to anaerobic oxidation of methane (AOM) triggered by gas seepage, gas emissions at the seafloor at 396 m water depths are not only related to the warming of bottom water and the potential shift in the gas hydrate stability zone (Berndt et al. 2014). The findings suggest a long history of methane seepage, which clearly weakens the hypothesis of recent global-warming-induced hydrate decomposition.

Gas-related seismic features occur at the upper slope and outer shelf in varies water depths (Ker et al. 2014; Sarkar et al. 2012; Rajan et al. 2012) and gas emissions occur not only at the upper boundary of the GHSZ (Westbrook et al. 2009). Typical hydrocarbon seep-related bacterial mats were observed at the shelf (Knies et al. 2004). Elevated bottom-water methane concentrations and the stable carbon isotope composition of methane in the water column indicate seepage at the shelf and within the fjords of Spitsbergen (Damm et al. 2005; Gentz et al. 2013).

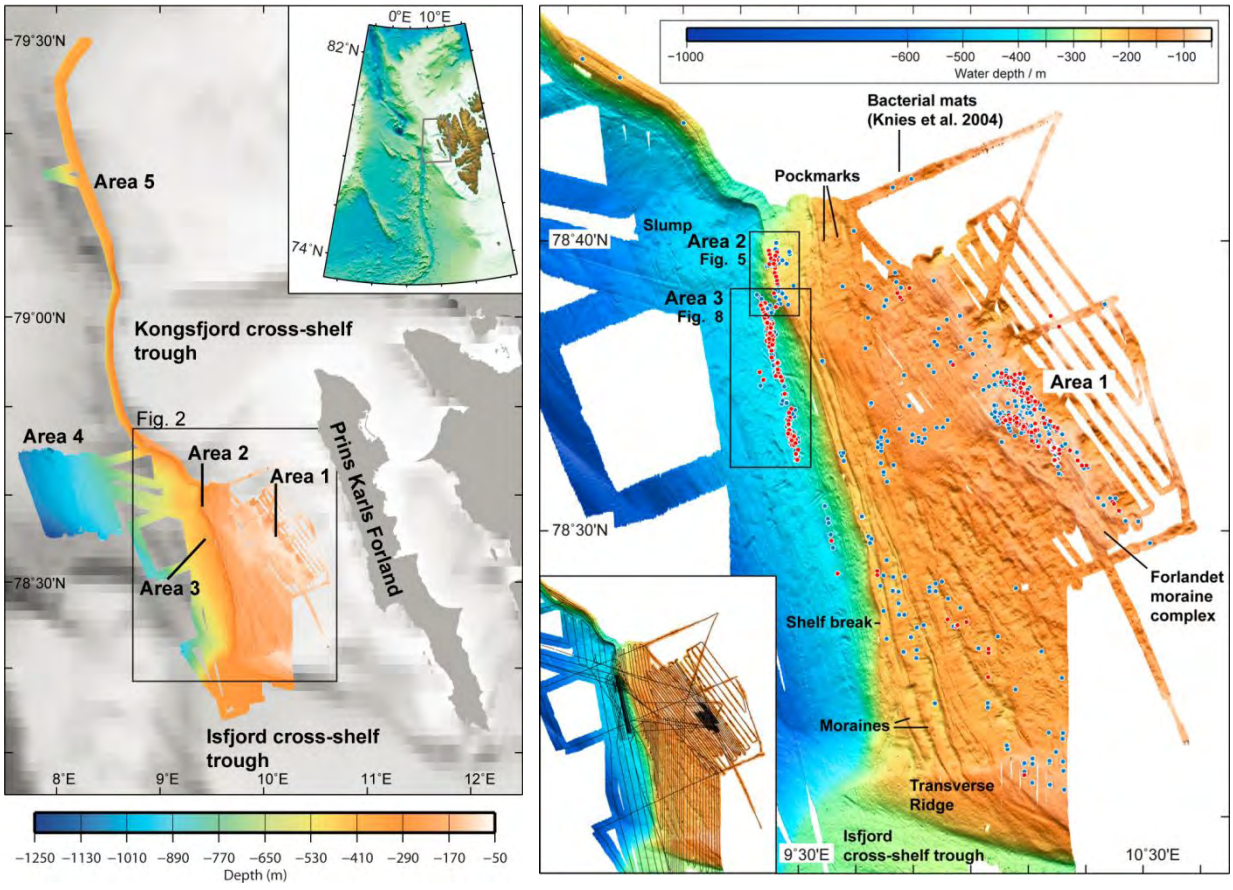

Fig. 6: Location of investigation by the R/V HEINCKE Cruise HE387 at Prins Karls Forland (left) and multibeam bathymetry and location of gas flares explored during summer 2012 as picked from EK 60 echosounder records separated in 3 regions (from Sahling et al. 2014).

A widespread investigation of gas emissions at the Prins Karls Forland margin and shelf was performed during R/V HEINCKE Cruise He387 in late summer 2012 (Fig. 6). Gas emissions were mapped, sampled, and quantified. Hydro-acoustic mapping revealed that gas emissions were not limited to a zone just above 396 m water depth and occurred widespread between about 80 and

415 m water depth, which indicates that hydrate dissociation might only be one of several sources for active hydrocarbon seepage in that area. Gas emissions were remarkably intensive at the main ridge of the Forlandet moraine complex in 80 to 90 m water depths, and may be related to thawing permafrost (Sahling et al. 2014).

Focused seafloor investigations were performed with a remotely operated vehicle (ROV). Geochemical analyses of gas bubbles sampled at about 240 m water depth as well as at the 396 m gas emission sites revealed that the vent gas is primarily composed of methane (> 99.70 %) of microbial origin (average $\delta^{13}C$ =−55.7‰ V-PDB). Estimates of the regional gas bubble flux from the seafloor to the water column in the area were achieved by combining flare mapping using multibeam and single-beam echosounder data, bubble stream mapping using the ROV-mounted horizontally looking sonar, and quantification of individual bubble streams using ROV imagery and bubble counting. The estimates by Sahling et al. (2014) show that gas emissions at the margin west of Svalbard were in the same range of magnitude as bubble emissions at other geological settings. The quantification which forms a baseline for the year 2012, can be used to calibrate models predicting hydrate decomposition at present and in the future.

2.3 Objectives of the Cruise

The main objective of the HEINCKE cruise was to perform exploration along the continental margin of Spitsbergen and the Barents Sea for gas emission sites. The concentration of gas flares west of Prins Karls Forland seem to be an exceptional place for this type of geosphere-hydrosphere interaction and there might be more places of strong gas exchange. The improvements in acoustic methods in recent decades led to a significant advance in finding gas emissions by acoustic anomalies in the water column. However, compared to satellite-based investigation of land areas, sea-floor mapping is a time-consuming work that is highly dependent on good weather and the water depth. Systematic sonar surveys around Svalbard and in the Barents Sea are therefore fragmentary. Since R/V HEINCKE is well equipped with modern sonar systems to contribute to the incomplete knowledge about gas release from shallow subsea-floor and potential from dynamic changes in gas hydrate deposits. In addition to the mapping we performed investigations on methane distribution in the water column and the air to increase our knowledge about gas seepage in the area. Sediment sampling by gravity corer, minicorer and van Veen grab and measurements of pore water and gas composition should give us further indication for seepage –related processes.

Main questions have been: Are there more areas of strong gas release from the sea-floor? In which sediments or at which geological settings are gas emission sites existing? Can we confirm an exchange between seawater and air? Are there typical pattern of gas emissions and what about the composition of gases at gas vents from different areas around Svalbard?

3 Cruise Narrative

(G. Bohrmann)

Tuesday 25 August:

R/V HEINCKE left the harbor of Tromsø on 08:00 exact time after three days berthing at Pier 24 located very close to the Tromsø University. The vessel came into the harbor on Saturday 22 August and change of the scientists and the loading happened on Monday 23 August. A track from Germany brought several boxes and equipment for the HE450 cruise and loaded equipment from the HE499 including a 20' Container to be transported back to Bremen. Embarkation of ten scientists took place for cruise HE450. Seven scientists from MARUM, Dr. Wei-Li Hong and Haoyi Yao from the Centre for Arctic Gas Hydrate, Environment and Climate (CAGE), UiT, Norway, and Marta Torres from College for Ocean, Atmosphere and Earth Science, Oregon State University, USA are the team for the next 14 days onboard. After the vessel started from the pier the safety officer introduced the new scientific crew to all safety rules onboard the ship. The vessel steamed through the fjords in northernmost direction and changed to a course towards west after free water was reached. The hydro-acoustic instruments of the ship started recording after we passed the 12 nm zone of Norway. After further 70 nm we reached the shelf break and followed the 450 m isobaths northwestwards (Fig. 7).

Wednesday 26 August:

Mapping overnight along the 450 m isobaths northwestwards using EM710, EK64 and the SES 2000 guided the vessel to pass over the omega-shaped slide scar of Bjørnøyrenna slide where also the well-known Håkon Mosby mud volcano is located in a deeper level of the scar in 1270 m water depth to the west. There was hope to find some gas emission sites for further sea floor sampling at the edge of the extensive Barents Island Trough Mouth Fan, however, no indication of gas emission could be observed.

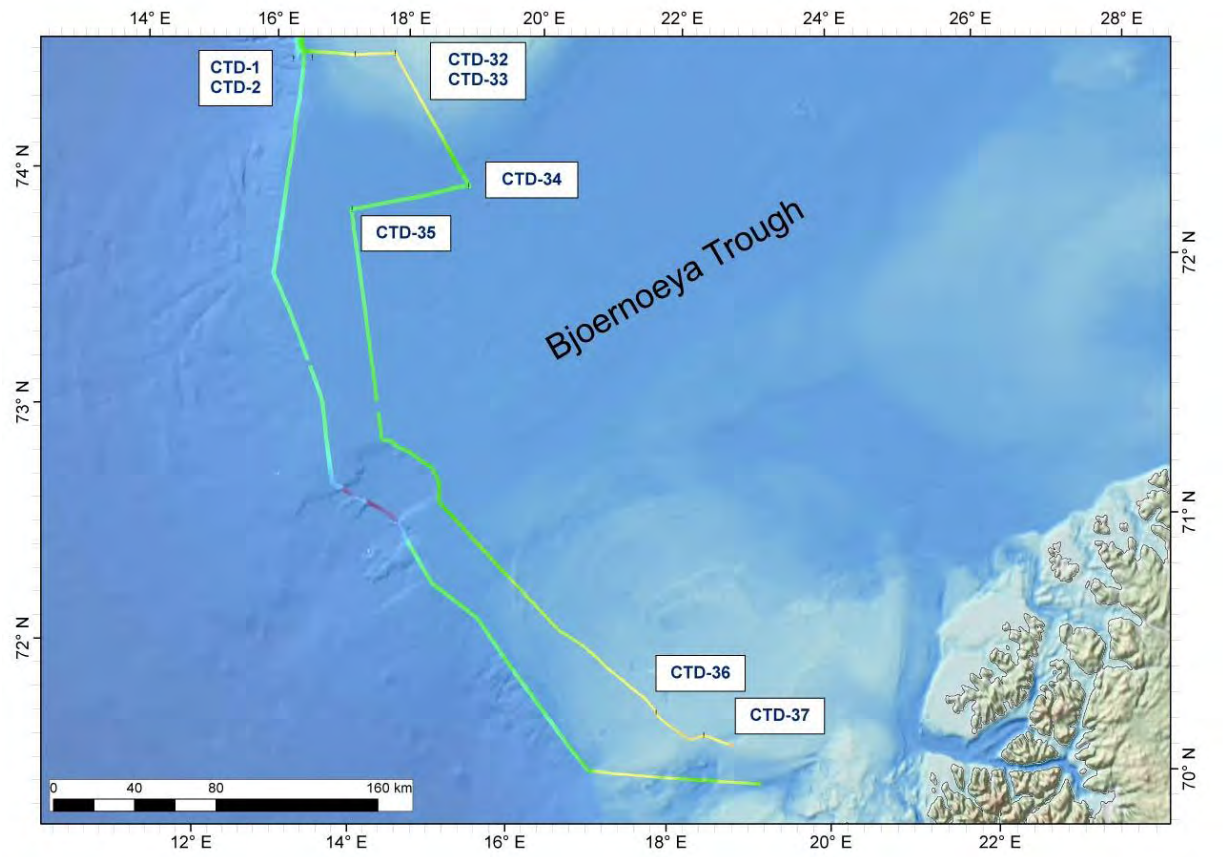

Fig. 7: Bathymetry lines and stations of Cruise HE450, southernmost part of three areas.

Thursday 27 August:

At 74°10'N we deployed our first CTD in 353 m water depth and shortly after that a second CTD (CTD-2) in 690 m water depth to acquire methane profiles from the water column. The shallow CTD-profile showed higher methane values, which is contributed from the shelf to the water column. After the stations have been finished we continued in mapping along the upper continental slope and took an additional CTD station where a flare was observed. As expected the methane concentrations in the lower water column close to the sea floor showed elevated values between 40-50 nmol/L. Along the shelf edge at latitudes west of Bjørnøya Island several flares were observed during R/V HEINCKE Cruise HE449 and our cruise which guided us to perform several tracks parallel and perpendicular to the slope during the night.

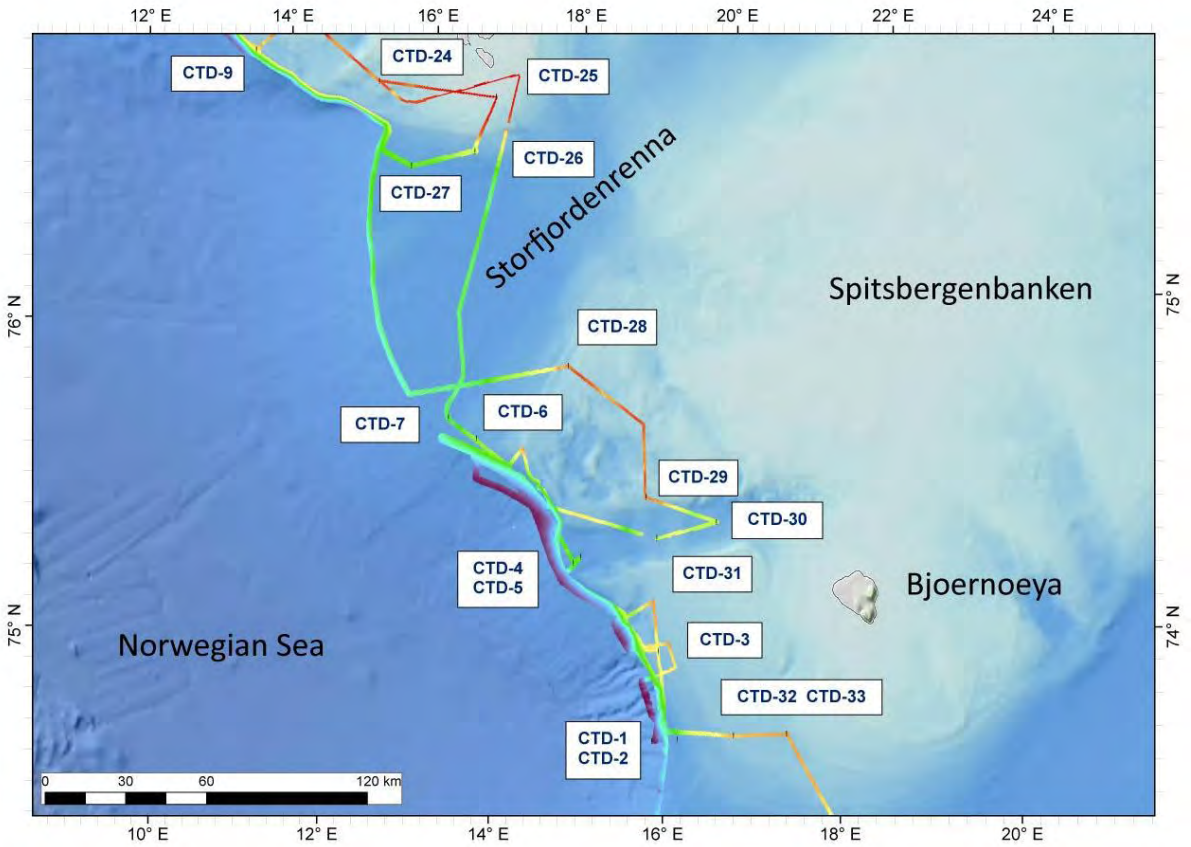

Fig. 8: Bathymetry lines and stations of Cruise HE450, middle part of three areas.

Friday 28 August:

This night's survey showed no more flare positions and the weather became increasingly windy. At 08:00 we started CTD-4 and CTD-5 in the Kveithola Trough Mouth Area where we had flare indications in 360 m from a former cruise. Hydro-acoustic indications could not be seen this time and the water column sampling revealed only very little increased methane concentrations at the bottom of 15-20 nmol/L. During early morning we had Beaufort 6 which increased to lower Beaufort 7 (Fig. 9). A second pair of water column sampling (CTD-6 and CTD-7) was performed during the afternoon north of Kveithola Trough and showed even less enhanced methane values close to the surface. Following the weather forecast and the actual wind situation we decided to cross during sea-floor mapping the Storfjord to the north and reached an area close to the southernmost tip of Spitsbergen on the shelf.

Saturday 29 August:

The course was probably too rough to find more gas emission sites using the acoustic systems of the ship, which changed on the shelf and immediately when we mapped with the ship on the shelf northwestwards flares have been observed. We followed a track covering several CTD stations at the Hornsund area where the highest methane concentrations have been measured during the cruise before (HE449). In comparison to the background values of 5 nmol/L in the upper water column stations at the Hornsund seeps and close by showed values of up to 15.6 nmol/L indicating most probably methane emission from the water to the atmosphere. We therefore recorded during the transect methane concentration in the air. CTD-8 was performed directly at the Hornsund seep to repeat a former measurement and CTD-9 sampled the shelf edge and added a seaward station to the Hornsund profile of HE449.

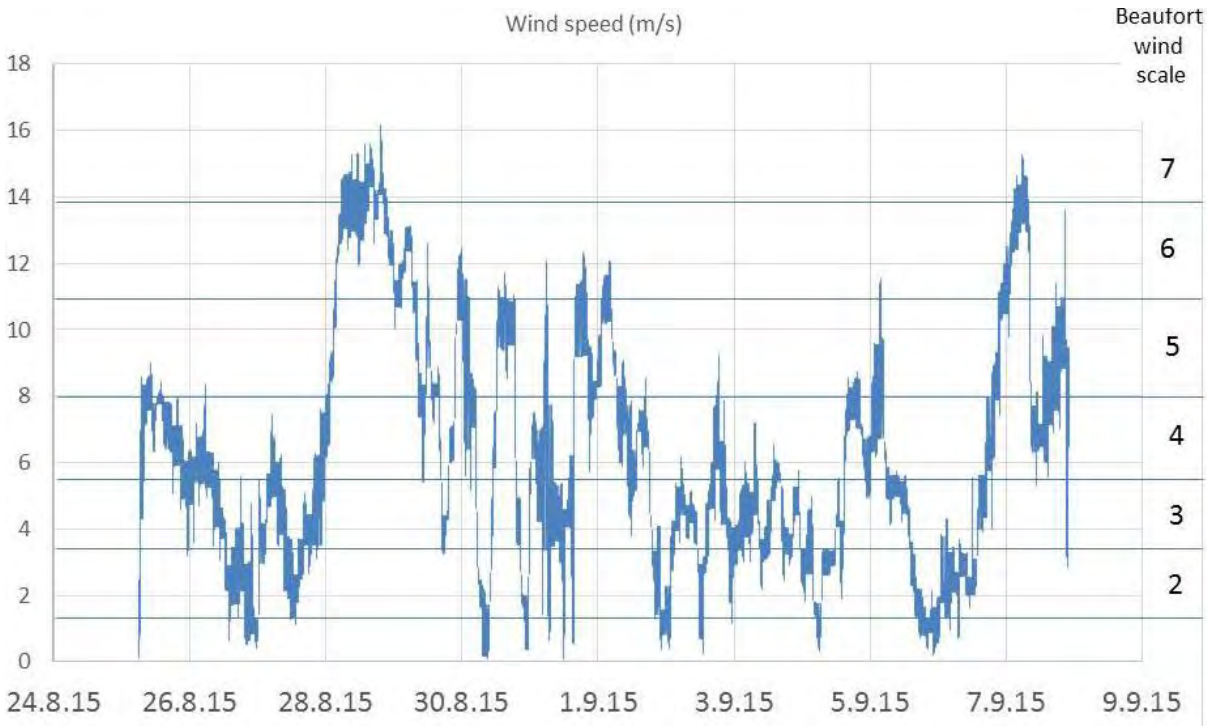

Fig. 9: Plot of wind speed during R/V HEINCKE Cruise HE450. Ten minutes values are plotted from the ship's meteorological data.

Sunday 30 August:

Based on the weather forecast from the day before the exploration strategy was to perform mapping northwards over the Prins-Karls-Forland gas seeps (PCF-GS) in around 400 m water depth and to test whether Vestnesa Ridge can be reached under acceptable weather conditions. Sunday's weather forecast showed, however, too much wind over Vestnesa Ridge (Beaufort 6), so that we reject this plan and developed a plan for station work 40 nm southward. The mapping during the night showed some flares in an area in around 400 m water depth at the upper slope of Isfjordbanken Margin which became the new target. After having taken two CTD stations in the northern Isfjorden Trough Mouth Area, CTD-10 in 300 m water depth and CTD-11 in 660 m water depth, R/V HEINCKE steamed to the area where the new flares have been found in the night before. Unfortunately, the weather was too rough (Beaufort 6) to take a gravity core and we only took a grab sample for sampling the bottom sediment. A large portion of cm-sized pebbles were mixed with soft sediment lumps which gave no hope for good gravity coring at that site. We extended the multibeam lines by five parallel

lines parallel to the slope and we hoped that the processing of the data will give us more information for sampling when coming back to the area during the later cruise. The night's mapping course brought us along the Isfjorden Trough Mouth Fan to the north over the margin of PCF to the Kongsfjord.

Monday 31 August:

Since the weather data showed strong winds in our potential sampling areas west and south of Spitsbergen we decided to search for gas emission sites in the wind-protected area of the Kongsfjord and Krossfjord, where no flares have been reported up to now. By moving with the ship to the east we found several flares and turned in front of the Kongsbreen glacier back to the west. Since there was space at pier of Ny Alesund beside an old sailing ship we decided to visit this northernmost settlement for two hours. We have been impressed by all of the town which is above all a research base of many nations mostly for atmospheric and climatic research and geophysics. We could visit the German Koldewey Station of the AWI and could take samples, which have to be transported back to Bremerhaven constantly cooled. After this unusual and unexpected break of the research work on the vessel we took CTD-12 at the deepest part of the Kongsfjord in 360 m water depth, during which we recorded a gas emission site close to the CTD-station (CTD-12) and took this site as a new location for a mini-corer (MIC-1) and gravity corer (GC-1). Both worked successfully and pore water and gas samples have been taken. The lithology of the 3.6 m long core was dominantly composed of silty clay, partly laminated in the upper part. Dropstones of various size and composition have been intercalated and dominate the lithology in few horizons.

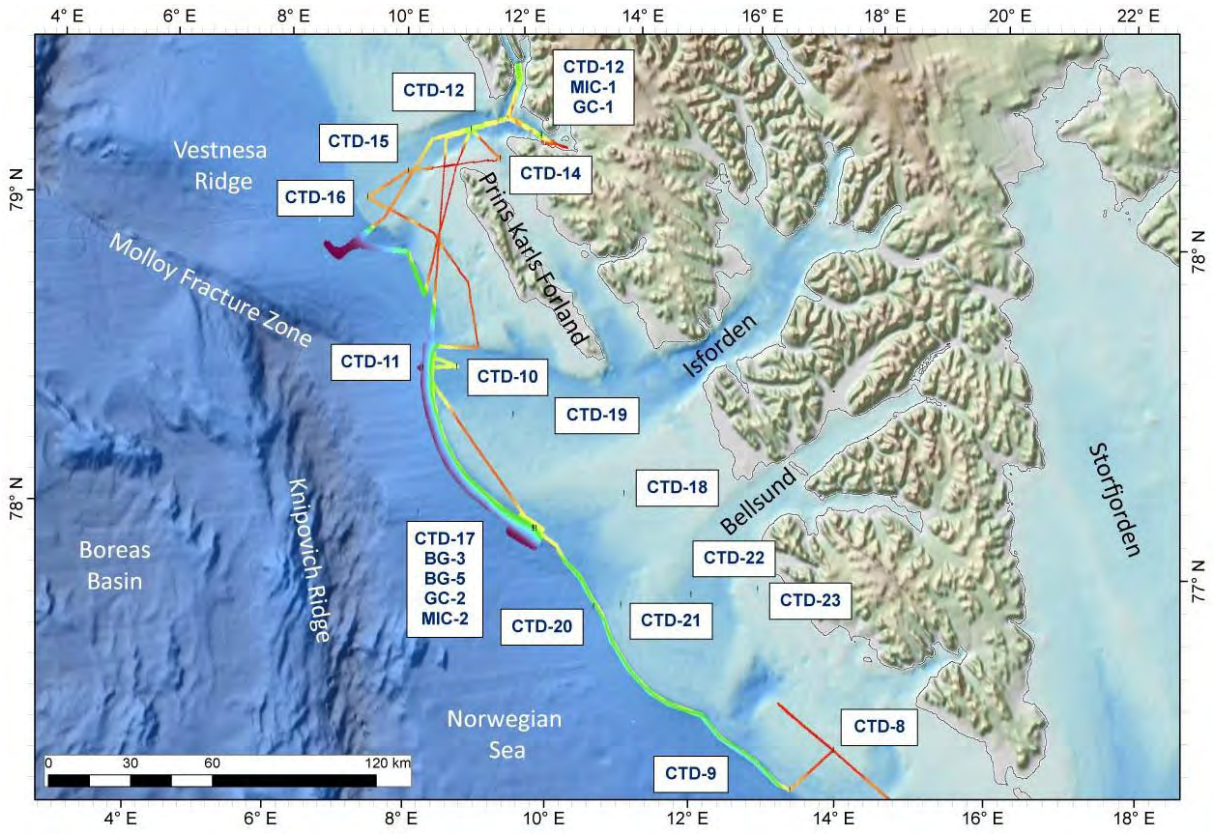

Fig. 10: Bathymetry lines and stations of Cruise HE450, northernmost and main area of three regions.

Some mapping tracks were performed within the Krossfjord, where no methane bubbles have been recorded in the water column. The second half of the day was very sunny until late evening and showed us wonderful insight into the glacial landscape and the geology surrounding the fjords.

Tuesday 1 September:

During the night's mapping on the way to Vestnesa Ridge we recognized that the weather became too bad for taking sediment cores. Three cores in and between well-known pockmarks on the ridge were planned to sample gas hydrates, however, this program was rejected. We decided to work closer to Prins Karls Forland where the wind speed was less. A NW/SE profile along the 400 m isobath covered the dense gas emission sites described by Westbrook et al. (2009). In order to finalize the water measurements for methane in our northernmost area, we decided to perform 4 CTDs along a line within the Kongsfjord cross-shelf trough. CTD-14 of that profile was placed in Forland Sund to document the contribution of methane from this broad passage, between mainland Spitsbergen and the Prins Karls Forland. The westernmost CTD of the profile (CTD-16) was placed in the Kongsfjord Trough Mouth area. The following hydro-acoustic mapping we took over the Forlandet moraine complex where many gas emission sites in about 85 m water depth have been found during Cruise HE-387. Gas emission sites have been very active as before and could be recorded by EK60 as well as by EM710 sonars. The ship moved afterwards to the west and followed the margin at around the 500 m isobath and added an additional line in the deeper slope to extend the multibeam map of that part of the margin.

Wednesday 2 September:

In the morning we reached at 08:00 the area at the margin in 390 m water depth where several flares have been observed some days before when we headed to the north. We started to take 3 grabs to test the sediment composition at various positions and had to recognize, that pebbles of various diameters up to fist-size were to be found on the seafloor location. Since the ship could use the online acoustic image of a flare for navigation we took a gravity corer and sampled just some meters beside a bubbling area. The sediment core of 1.90 m recovery was well preserved, however, gas hydrate was not sampled. Unfortunately the winch stopped 2 times and the wire which came between some rolls loosened and formed several loops. Since this operation was too dangerous, the decision came to the point that the gravity corer should not be used anymore during this cruise. Unfortunately, this was a serious consequence for our cruise because gas hydrates could not be sampled anymore. After the core we took a CTD-station close by, moved to the gravity core position again and sampled a minicorer (MIC-02). Two more CTD stations (CTD-18 and CTD-19) were taken in 100 m WD at the inner part of the shelf and in 218 m WD at the center of the Isfjorden Trough Mouth. Mapping for the night started from the last CTD station westwards and along the margin partly with 3 lines parallel to the margin.

Thursday 3 September:

After a long mapping night a series of CTD stations started from the deepest station at the margin with 500 m water column (CTD-20) over the outer shelf (CTD-21 in 200 m water depth) to the inner shelf (CTD-22 in 170 m water depth) and close to the Bellsund Banken (CTD-23 in 90 m water depth). From CTD-23 station the hydro-acoustic mapping started over the shelf back to the margin, where first a line northwestwards along the shelf break of the Bellsund Trough Mouth Fan was performed. Further mapping guided the ship southeastwards back along a line at the upper slope. Today's weather was very calm so that the ship's speed of 10 knots could be used all the time.

Friday 4 September:
In the morning the sea surface was completely flat, showing no waves at all. The only waves were made by the ship itself which makes hydro-acoustic mapping very productive and we could continue in mapping with a speed of 10 knots. In the morning the ship left the margin and steamed over the outer shelf including the Hornsund gas seeps for measurements of methane in the air. This transect on the shelf parallel to the margin was made on Friday 28 September when the ship steamed in the opposite direction during high wind speed Beaufort 5 to 6 and higher methane concentrations have been measured in the air. The repetition of the measurements today under very calm sea state conditions should show the potential influence of the wind-induced waves on the methane concentrations in the air. Immediately when we steamed over the Hornsund gas seeps we recognized the well pronounced gas flares in the water column. At the end of the line we run CTD-24 in 175 m water depth. At the southern tip of Spitsbergen another CTD was performed in 50 m water depth. Two more CTD stations followed in the afternoon, CTD-26 and CTD-27. Both stations represent locations on the Storfjord Trough Mouth in deeper water of 370 m and 330 m. Mapping in the evening and night followed along the margin off the Hornsundbanken and to the south along the northern part of the Storfjord Trough Mouth Fan.

Saturday 5 September:
During early morning we crossed the Storfjord Mouth Fan to its southeastern rim and took CTD station 28. Further three CTD stations CTD-29, CTD-30 and CTD-31, were performed north and within the Kveithola cross shelf trough during the day. The mapping in the evening brought us first along the shelf break to the north were we stopped at night before mapping.

Sunday 6 September:
At very early morning on the way back we crossed to the south the Kveithola in the trough mouth area and have run the first CTD (CTD-32) around 40 nautical miles to the south and steamed 10 nm to the east for taking CTD-33. The weather was very calm and allowed sight to far distance. We could have a wonderful view to the Island of Bjørnøya around 30 nm away. The sea surface was extremely flat and we could observe a group of whales with their fountains, coming closer during steaming of the vessel. Before we took the further two CTD stations (CTD-34 and CTD-35) we had to steam 30 nm to the south and immediately after the last station we started the mapping to the south over the Barents Sea Trough in direction to the Barents.

Monday 7 September:
Sea floor mapping became difficult because of the sea state. The sea surface became rough during wind speed of Beaufort 6 and 7. We had to cancel the first two CTD stations of the day because of high waves. We also had to shorten the track on the way to the south. During afternoon the sea state became more calm, so that we could perform the last two stations of the cruise CTD-36 and CTD-37. In the evening we reached the border of our research area and we stopped recording the sonar systems.

Tuesday 8 September:
R/V HEINCKE reached the fjord systems in northern Norway, which form the passage to Tromsø. The ship entered the harbor of Tromsø in the morning and berthed at 08:00 at the same place pier 24, where we started exactly 14 days ago. The ship steamed 2,516 nm and we mapped about 2,400 nm using multibeam EM710, fish finder EK60, and subbottom profiler SES2000. We took 37 CTD stations,

5 grab samples, 2 gravity corer and 2 minicorer stations. R/V HEINCKE Cruise HE450 was a successful cruise.

4 Hydroacoustic Work

(P. Wintersteller, C. Ferreira, C.-W. Hsu, M. Loher)

During cruise HE450 several acoustic devices were used to map the water column, seafloor surface morphology and sub-bottom sediment layers. A sketch of the hull-mounted positions of echosounders can be found as addendum to this chapter.

Interferences between the different echosounders occurred, but are bearable with respect to post-processing. For several reasons interferences clearly increase with bad weather conditions.

All georeferenced data are based on a geographic coordinate system (WGS84) and large overview maps are displayed in a projected coordinate system (Polar Stereographic). For small scale maps a UTM projection (ETRS 1989 UTM Zone 32N) was used.

4.1 Multibeam Echosounder EM710

4.1.1 System Setup

The Kongsberg EM710 is a shallow to mid-water Multibeam Echosounder (MBES) operating between 70 and 100 kHz and optimal depth range from 10 to 1200 meters. With a transducer configuration of 1 by 2 degrees (TX/RX) this system has 200 beams, with 400 soundings in high density mode, measuring both bathymetry and backscatter. The Water Column Data (WCD) were recorded to detect and analyze gas seepage sites.

The system was operated with a maximum swath angle of 120 degrees except of Survey 9 to 11 where swath width was set to 130° in automatic ping mode. Between the surveys CTDs were carried out and used to calculate Sound Velocity Profiles (SVP) that were inserted in the acquisition software Seafloor Information System (SIS) version 4.1.2 (from October 2013). The Surface Sound Velocity (SSV) was measured by the C-Keel sensor which is a very important parameter because it is used to calculate the initial direction of the beams transmitted/received. The logging of the data was set to generate a new file every 10 minutes with the water column in a separate file. The filter settings used were “Spike Filter Strength” as STRONG, “Range Gate” as SMALL, “Phase Ramp” as NORMAL, “Penetration Filter Strength” as WEAK, and the activated additional filters were: “Slope”, “Aeration”, “Sector Tracking”and “Interference”. Roll, Pitch and Yaw corrections were active during the whole cruise.

During the surveys the EM710 experienced a few crashes (acquisition software and/or processing unit) but was otherwise stable nearly the whole cruise. The C-Keel sensor worked flawless until about half of the cruise and then stopped working for a few days. In fact, it had several issues delivering data during the cruise. Cleaning and maintenance were done by the chief engineer on September 4. The probe seems to work reliable since then. The wobbling issues found on cruise HE387 (Sahling, 2012) are still visible in the data.

In total 4346.84 kilometers were surveyed with an average speed of 7.52 knots during 312.23 hours generating 1856 files. The overview map (Fig. 1) shows the total coverage of the HE450 MBES data.

4.1.2 Bathymetric Processing

The open source software package MBSystem version 5.4.2213 (Caress and Chayes, 1995) has been utilized to post-process the bathymetric data. Besides manual editing a tide correction as well as partial sound velocity correction has been applied. Currently the preliminary dataset, as shown e.g. in chapter 4.5, is roughly cleaned and need further detailed investigations before being published.

4.1.3 Processing of the Water Column Data (WCD)

A key aim of HE450 was the investigation of active gas emission sites on the seafloor where gas bubbles can be hydroacoustically detected in the water column. For this purpose, the water column data generated by the EM710 as well as the signal from the EK60 were monitored constantly and the occurrences of flares were noted in a GIS software (Global Mapper) “on the fly”, mentioned as online observations in Figure 11 below.

Storage of the water column data (.wcd files) allowed post-analyses of detailed flare occurrences (flare picking) in FM Midwater and FM Fledermaus . The workflow used is shown in detail in Figure 11. The picked flare source-points were then imported in Global Mapper and serve as sites of interest for further hydroacoustic surveys, sediment sampling or CTDs. The picked complete flares are used for visualization and potential quantification of the flare site.

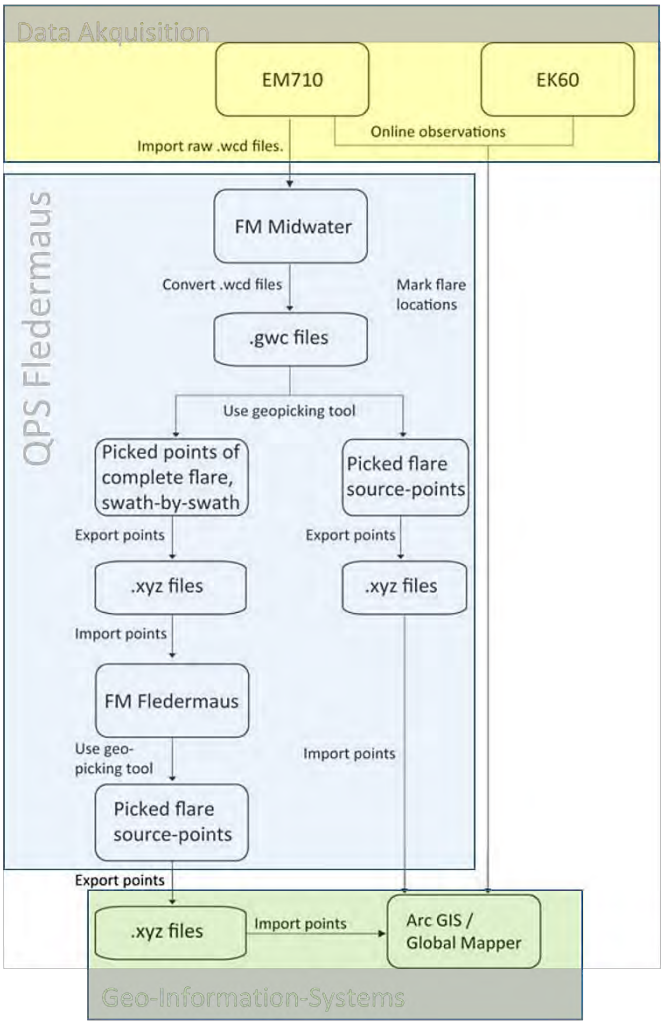

Fig. 11: Work flow of flare mapping during HE450 cruise.

4.1.4 Statistics

In total 59.3 GB of EM710 bathymetry-data were recorded in 2373 *.all files, almost continuously between the 25th of August and the 7th of September. This includes partly station time. Water column was recorded in parallel to in total 1857 *.wcd files, with a size of 260 GB.

4.2 Singlebeam Echosounder EK60

4.2.1 System Setup

The hull-mounted split beam echosounder KONGSBERG EK60 was utilized to aid discovering seep sites with gas emission during the cruise. To avoid further interferences just the 38kHz transducer ES38B, with 7 degrees beam angle was activated. The split beam principle is used to find the position of individual targets in the transducer beam, compensate for the beam pattern and calculate corrected target strength values. In total 4 out of up to 7 possible split beam transducers are installed on R/V HEINCKE. There frequencies are 38, 70, 120 and 200 kHz. According to the description the 38kHz transducer is able to observe single fish down to 1000 m water depth. Due to large distances and other main purposes the survey speed during this cruise was mostly around 8-10 kn. Therefore the 38 kHz single beam echosounder has clear advantages in along-track-resolution compared to the multibeam echosounder EM710. The ping rate of the single beam sounder is higher since the 2-way travel times are short at nadir (e.g. Fig. 12).

Settings during the cruise:

Pulse length	256 us
Sample interval	64 us
Band width	3.67 kHz
Power	1000 W

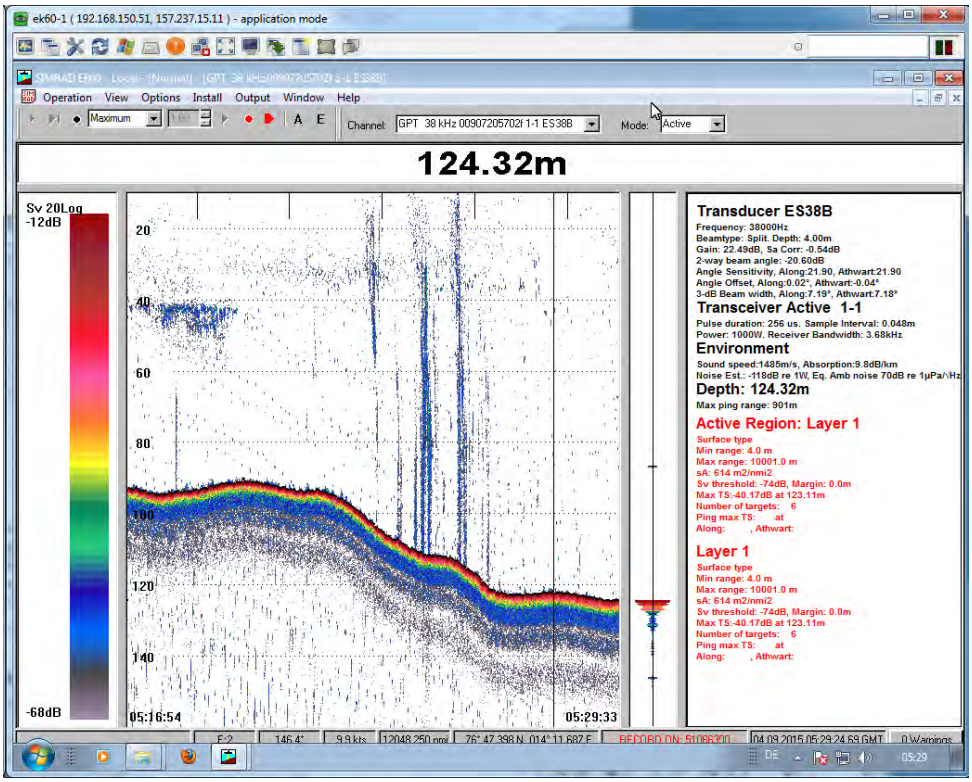

Fig. 12: Screenshot of along-track gas flares in the water column at about 115 m WD.

4.2.2 Statistics

In total 207 GB of EK60 data were recorded in 6372 files, continuously between the 25th of August and the 7th of September. This includes station time.

4.3 Parametric Subbottom Echosounder SES2000

The INNOMAR SES2000 is used to study subsurface structures (different sedimentological units, tectonic structures), to recognize gas charged sediments (blanking zones) as well as to investigate particular seafloor morphologies (pockmarks, sediment waves, glacial deposits) in detail.

4.3.1 System Setup

The SES2000 medium is a sub-bottom profiler (SBP) which utilizes the parametric effect based on the non-linear relation of pressure and density during sonar propagation. A primary high frequency (HF) wave (of about 100 kHz) is used to create a so-called secondary low (about 6 kHz) frequency (LF). Throughout the cruise the SES200 was continuously recording and no problems were encountered.

Table 3: Settings during HE450.

Transmit:	
LF Frequency: LF Pulses: LF & HF: HF Signal Damping:	6 kHz 1 Auto Gain Control ON
Processing:	
Soft TVG: Median Filter: Normalize Gain Reduce Noise	0.5 dB/m ON ON ON
Range:	
Default: Auto Range Start: Use of LF-Water Depth:	A range of 100 m was recorded for most of the cruise. ON ON
Threshold:	
LF Mode: HF Mode:	Logarithmic with: Min Level = 1; SRange = 4 Logarithmic with: Min Level = 4; SRange = 8
Depth:	
Detection Sensitivity LF: Detection Sensitivity HF: Draw LF WD-Line: Bottom Averaging	40 % 40 % ON On Level 7

4.3.2 Data Analysis

The online view of the SES2000 displayed the LF and HF signal in different panels (Fig. 13). Due to the automatic seafloor detection, data was always displayed over a range of 100 m and automatically adjusted when changes in the water depth occurred. The data output was stored as ".ses" and ".raw" files and could be replayed in the ISE software, available onboard.

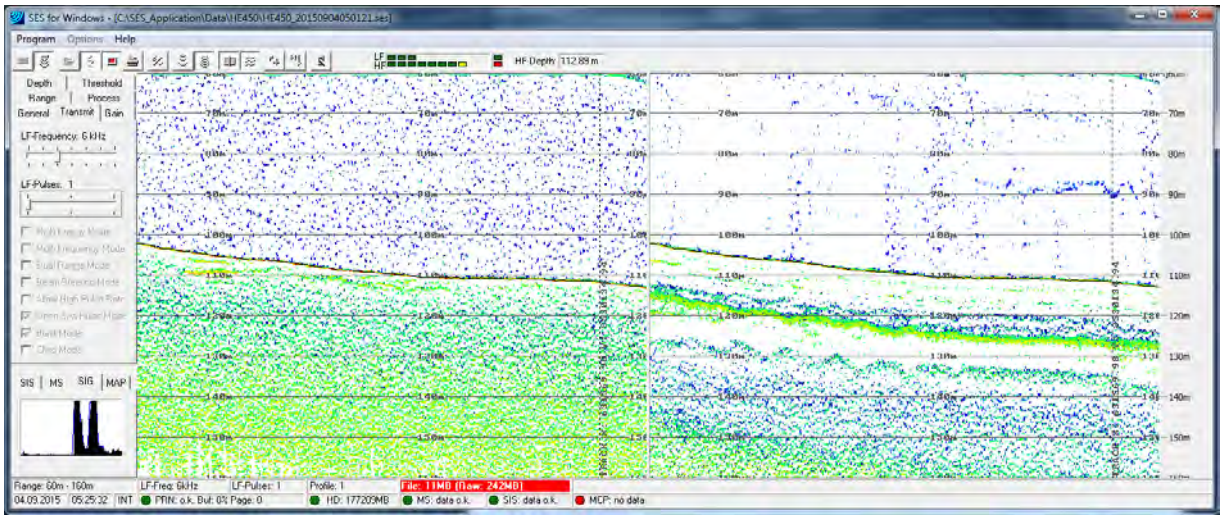

Fig. 13: Online screenshot of the SES2000 (31/09/2015 at 05:26). The low-frequency (LF) panel on the left shows deeper penetration but lower resolution compared to the high-frequency (HF) on the right. In the HF panel, gas plumes are visible as faint anomalies trending vertically in the water column.

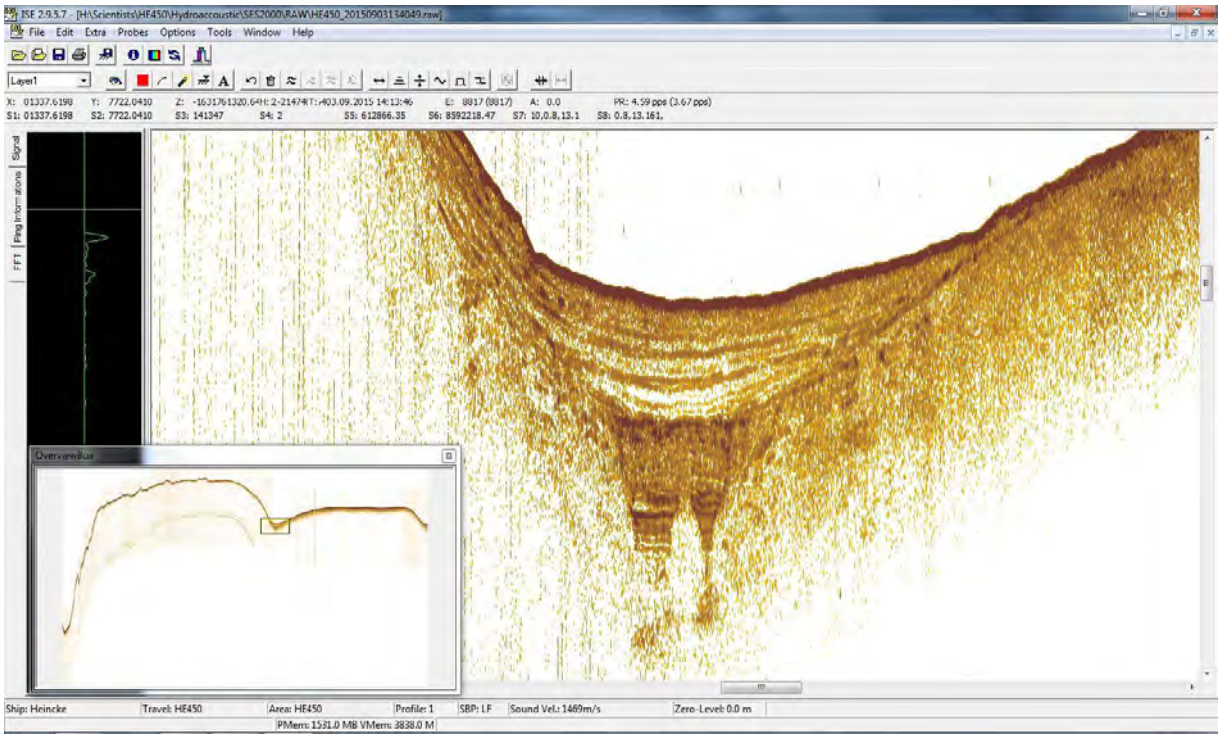

Fig. 14: Screenshot of the ISE software where the SES2000 sub-bottom data is replayed and post-processed. The image shows buried subglacial channels in a trough along the shelf-edge, recorded during survey 10.

In principal, glacially influenced sediments are difficult to penetrate with parametric SBP devices due to high signal attenuation and scattering in non-layered deposits and relative low energy source levels for the low-frequencies. However, Figure 14 is a nice example of filled troughs and subglacial channels in the Kongsfjorden.

4.3.3 Statistics

In total 102 GB of SES2000 data were recorded in 395 files (*.ses and *.raw), almost continuous between the 25th of August and the 7th of September. This includes station time.

4.4 Acoustic Doppler Current Profiler ADCP

The RDI Ocean Surveyor ADCP OS-150kHz transducer has a 4-beam phased array and is hull mounted with Beam 3 directing 45° (NE) towards starboard. The system runs with settings given by AWI/Fielax. Bin size has been changed during the cruise at 08:22 on the 5th of September, from 8 m to 5 m. The data acquired is relatively noisy due to parallel and unsynchronized recording of EM710 and SES data. Since the data has not yet undergone detailed post-processing for correcting heading, position and bottom-depth no preliminary data is shown here. Information extracted from the shipside database DSHIP will be utilized for this processing steps.

4.4.1 Statistics

Between the 3rd and 7th of September 95 Files, in total 843 MB, were recorded using the Teledyne RDI software package VMDAS.

4.5 Preliminary Results & References

According to the objectives of the cruise (see chapter 2.3) the major aim was to search for further gas emission sites along the Svalbard and Barents Sea shelf. With respect to the covered area first preliminary results after cruise POS449 and this one show a clear clustering of gas emission sites along the shelf.

Since the area of investigation is huge, we followed a first survey idea in crosschecking and extending the search conducted during POS449. Whenever possible our way led back to the shelf break which for several reasons was our choice to look at in detail. All maps below are shown in polar-stereographic coordinate system with central meridian 15° E and central latitude 70° N. Hillshades were created with 4 times exaggeration of the elevation value, within ESRI ArcGIS™.

4.5.1 Barents Sea Shelf (Kveithola Trough)

The most southern area of investigation started right after 12 miles distance from Norway mainland and led us, on the way back, over the famous long-term observed site of the Håkon Mosby mud-volcano-area. Nevertheless, the first evidence of gas in the water column was found north of it in the vicinity of Bear Island and the Kveithola Trough (Fig. 15). The area has been extensively investigated by Rebesco et al. (online 2016) with respect to seafloor-morphology and paleao-ice-streams. Gas emission sites in this area occur on the outer shelf between about 215 m and 350 m water depth. The outer shelf and shelf break is characterized by a hammocky belt throughout, also overprinting the grounding-zone of the Kveithola Trough Mouth (KTM, Fig. 15 close-up). Extended iceberg ploughmarks are visible there.

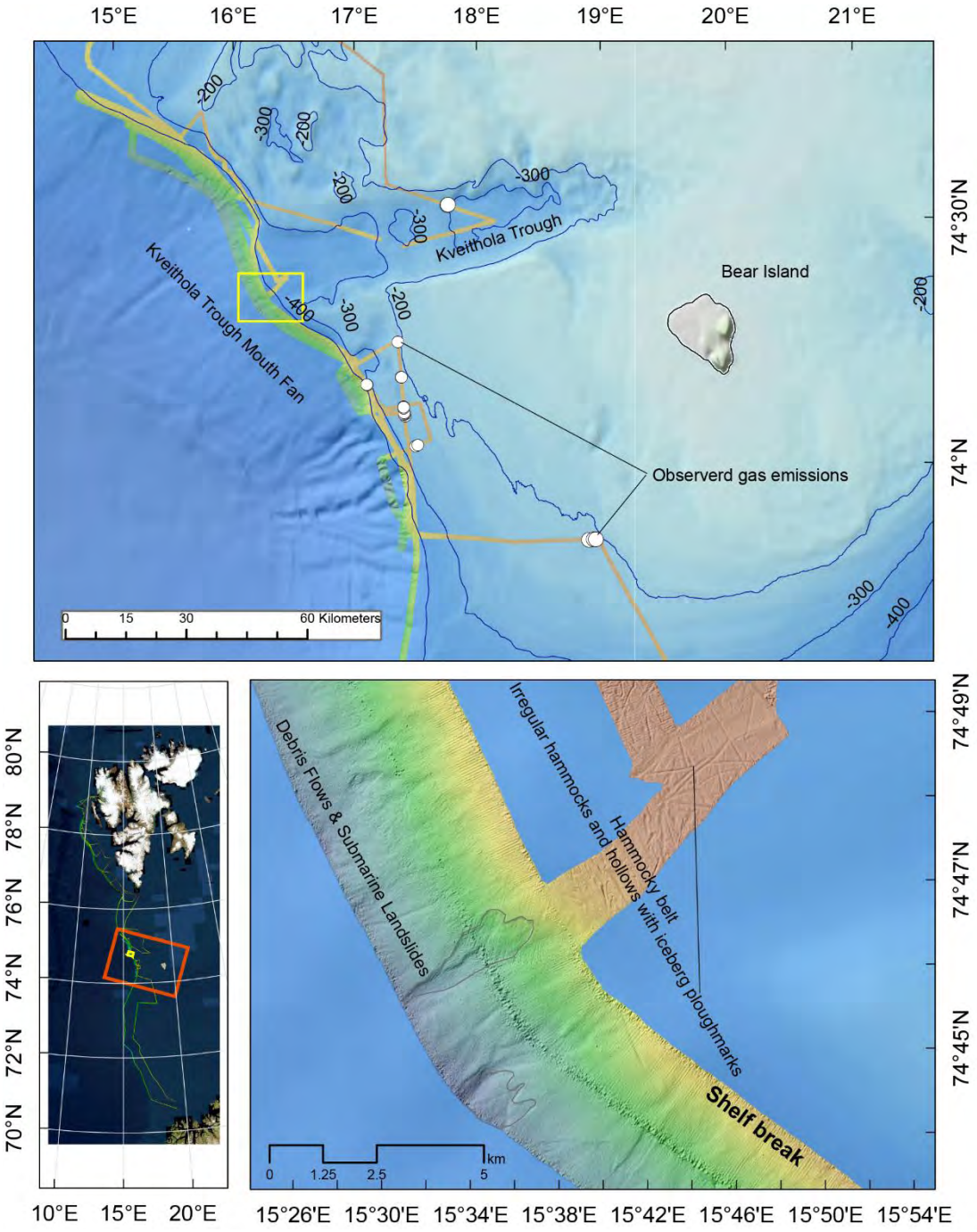

Fig. 15: Gas emissions and evidence of a hammocky belt/moraine along the shelf break and submarine landslides on the slope

4.5.2 South-Western Svalbard Shelf (Hornsund)

The area around Hornsund Trough is characterized by large gas emission sites (Fig. 16), pockmark like features along the outer shelf and shelf break as well as furrows or faults, striking parallel to the shelf break over long distances within the slope (Fig. 16 close-up). A dense pattern of gullies, channels and submarine landside-break-off edges is expressed on the slope, right below the shelf break.

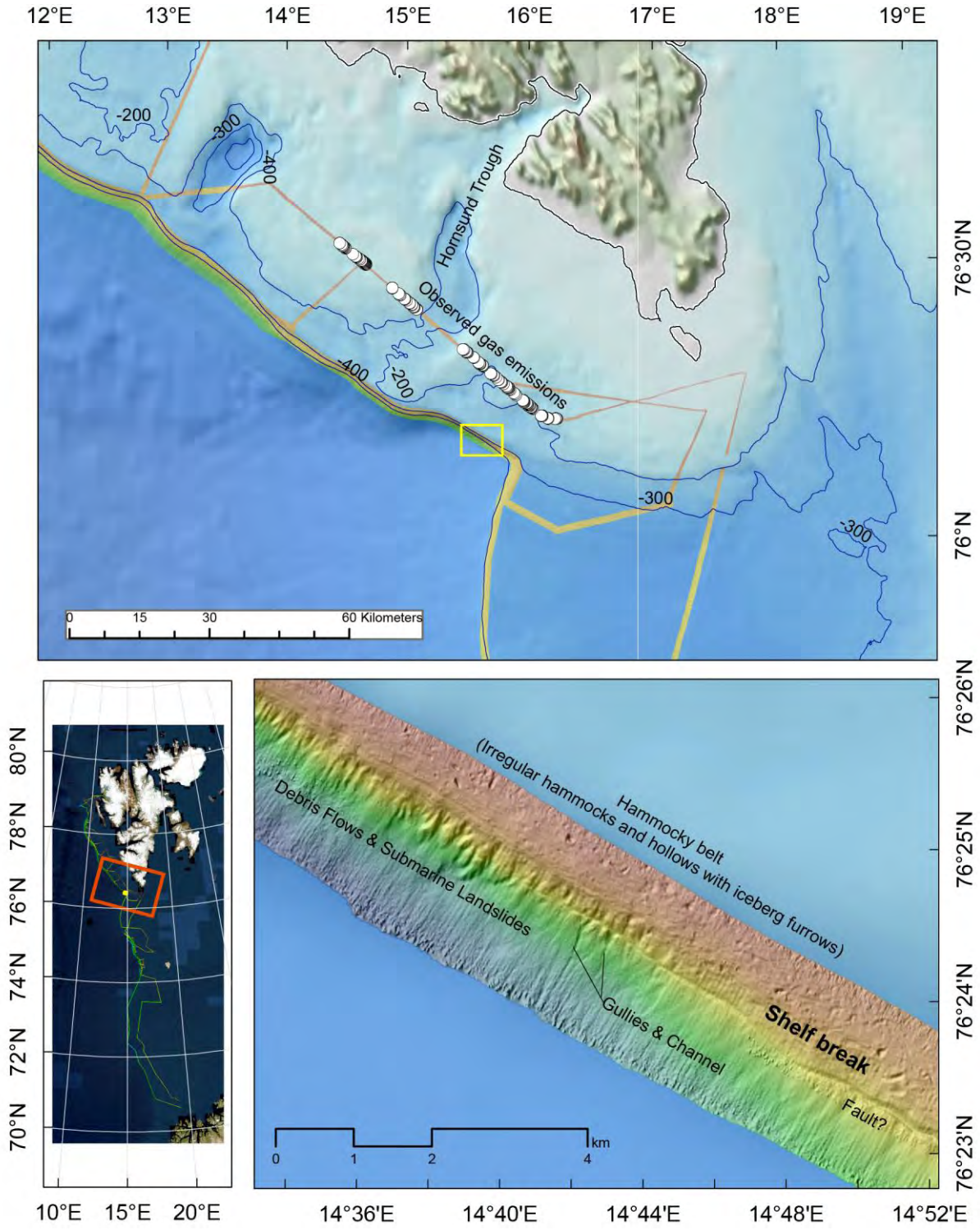

Fig. 16: The area around Hornsund Trough, its gas emission sites, pockmark like features along the outer shelf, break-off edges of submarine landslides, gullies and furrows (faults?) within the slope.

4.5.3 Central Western Svalbard Shelf (Isfjorden)

The most prominent gas emissions in this area are the well-known ones on the outer shelf off Prins Karls Forland but we also observed two positions at around 390 m WD between Isfjorden and Bellsund Trough (Fig. 17). Again the outer shelf shows evidence of grounded icebergs due to the presence of iceberg furrows, hollows and hammocks in the Isfjorden Trough Mouth and beyond. A pronounced system of gullies and channels is visible right below the shelf break.

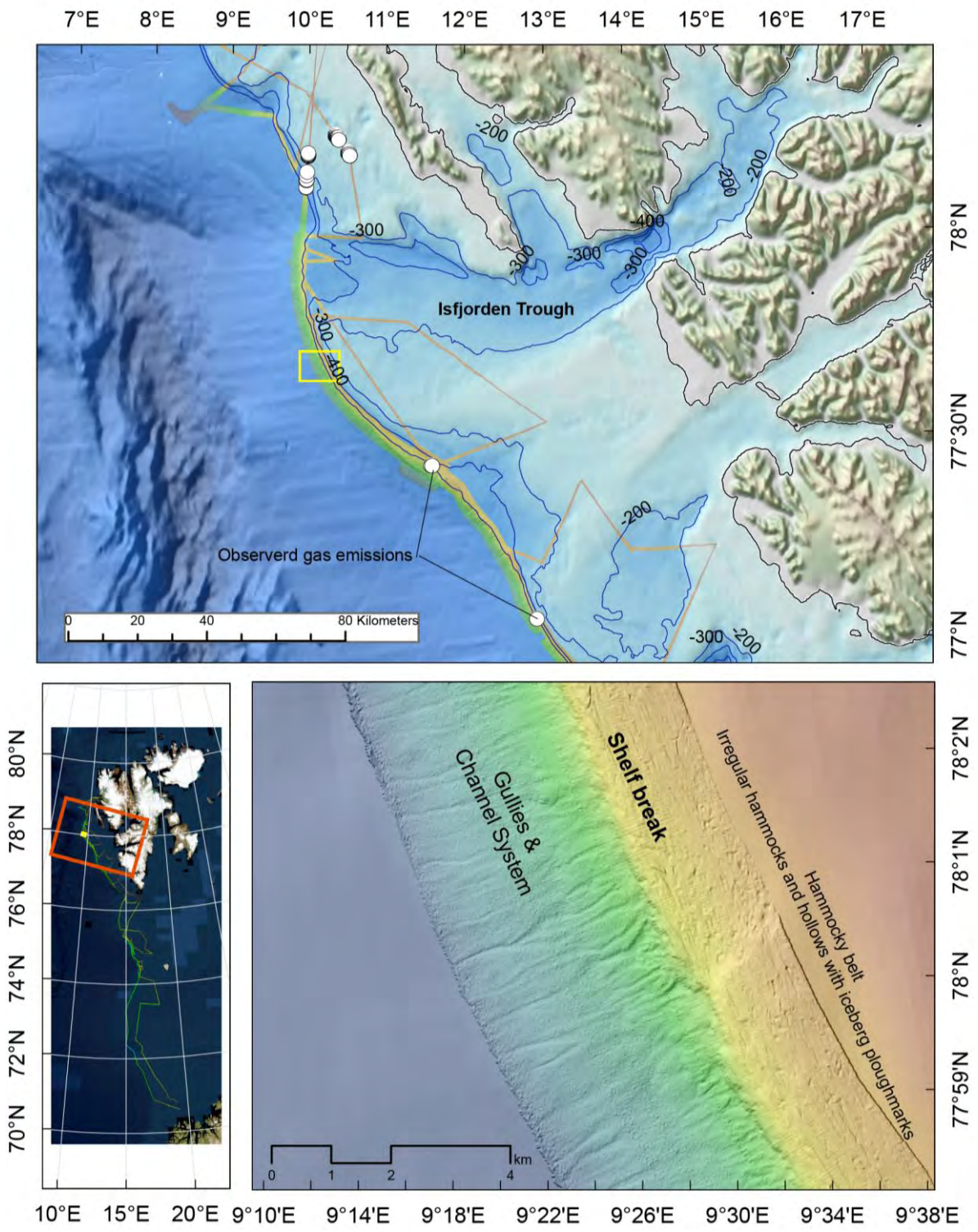

Fig. 17: Gully and channel system along the central West-Spitsbergen shelf with a prominent gas emission site off Prins Karls Forland.

4.5.4 North-Western Svalbard Region (Krossfjorden and Kongsfjorden Trough)

Gas emission observations between the Kongsfjorden Trough Mouth and eastward grounding-zone-wedge (GZW) and within the Kongsfjord are situated within 165 and 320 m WD (Fig. 18). Other than expected we could not find gas flares during the survey of the Krossfjord but glacial lineations on the

sides of the deepest area as well as two GZWs show evidence of relatively fast glaciation/deglaciations in former time (Ó Cofaigh et al., 2005).

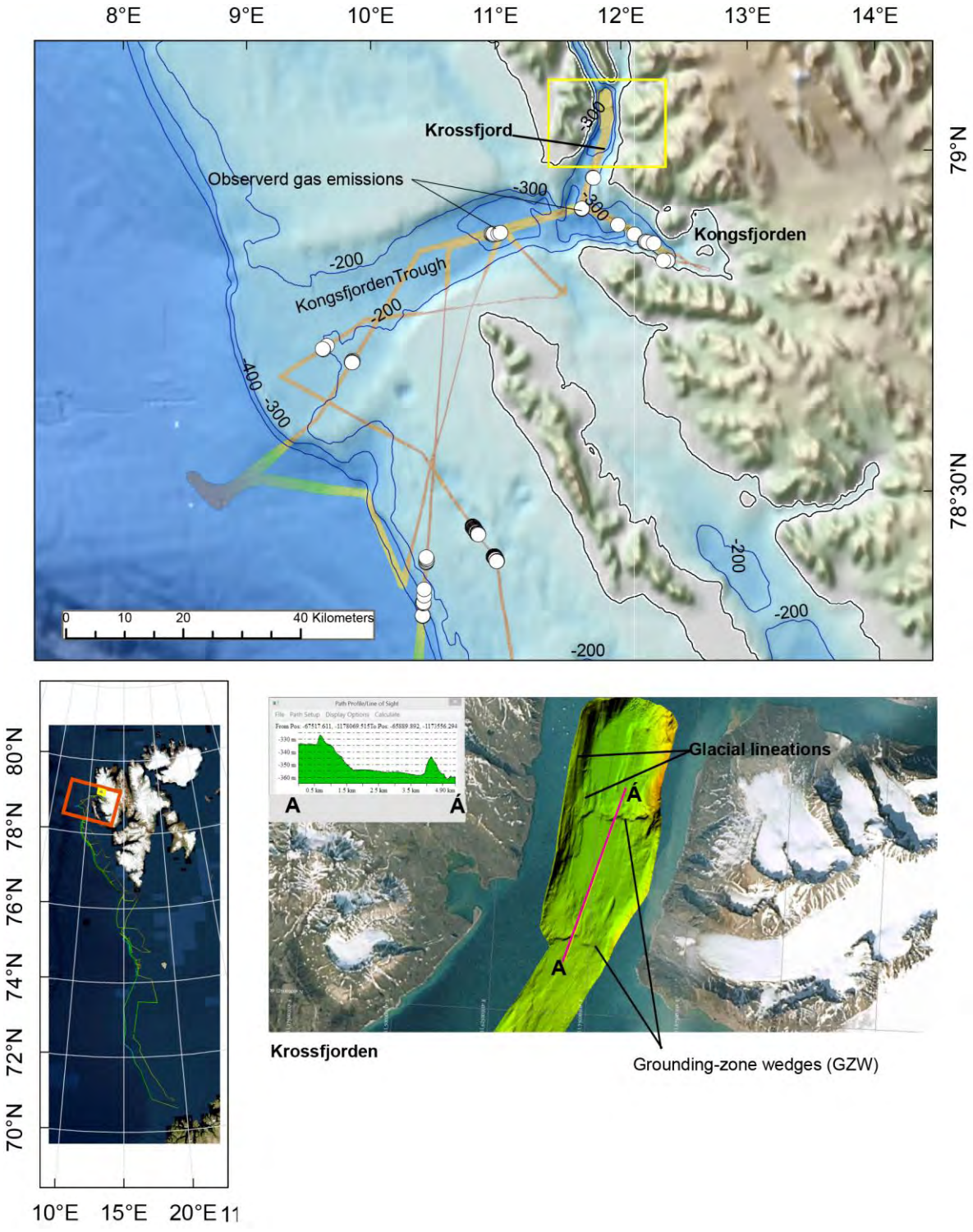

Fig. 18: Map of Kross- and Kongsfjorden and the Kongsfjorden Trough with the only observed gas emission positions on this cruise that lie within the troughs thalweg.

Addendum: Drawing of the positions of the echosounders on R/V HEINCKE.

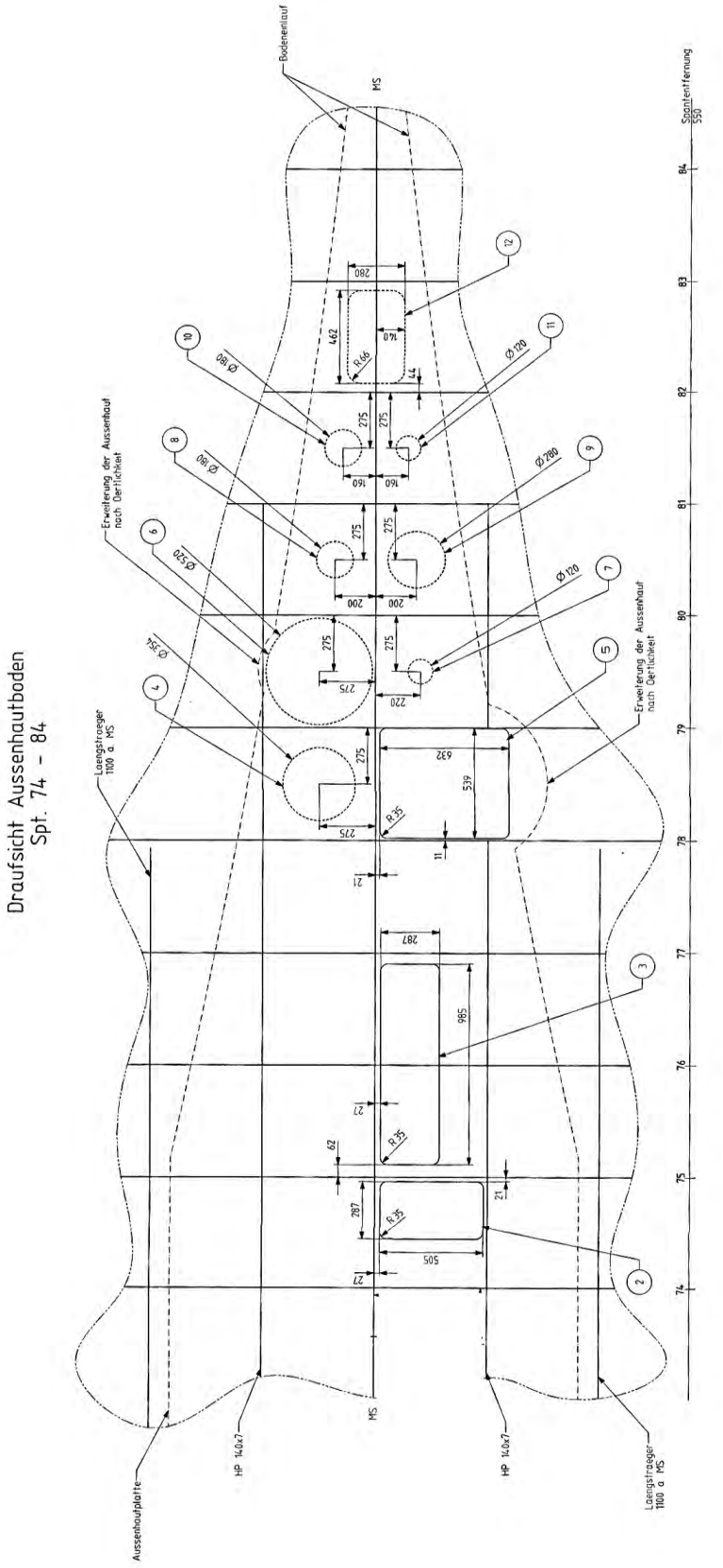

Pos.	Benennung
2	2 GRAD TX / RX
3	1 GRAD TX / RX
4	ADCP
5	SES - 2000
6	FISCHEREILOT EK60 38KHz
7	EM LOG
8	FISCHEREILOT EK60 120KHz
9	FISCHEREILOT EK60 70KHz
10	NAVIGATIONSLOT SKIPPER 50KHz
11	FISCHEREILOT EK60 200KHz
12	DOLOG SAM

Note: The R/V HEINCKE manual is currently outdated with respect to implemented sensors e.g. GPS devices. AWI and Fielax are aware of the circumstances and will take care near future.

5 Water Column Work and Air Sampling Program

(M. Torres, T. Pape, M. Lange)

5.1 Introduction

There is a growing body of data documenting that the continental margin west of Svalbard is prone to hydrocarbon seepage. The presence of gas hydrates (below ~600 m water depth) and free gas below the base of the gas hydrate stability zone is indicated by the presence of a bottom simulating reflector (Vanneste et al., 2005; Westbrook et al., 2009; Chabert et al., 2011). Gas emissions concentrated along a band at seafloor depths just above the 396-m isobath have been attributed to temperature induced gas hydrate dissociation in response to a warming trend of the bottom water of 1°C over the past 30 years (Westbrook et al., 2009). In addition to these well studied seeps on the Svalbard slope, gas-related seismic facies have also been observed on the upper slope and outer shelf (Sarkar et al., 2012; Rajan et al., 2012) and gas discharge has been mapped on outer shelf at water depths up to 150 m (Westbrook et al., 2009). Additional evidence for seepage on the shelf was provided by elevated bottom-water methane concentrations and the stable carbon isotope composition of methane in the water column (Damm et al., 2005; Gentz et al., 2013), as well as by remotely operated vehicle (ROV) observations of widespread occurrence of methane bubbling sites between about 80 and 415 mbsl (Sahling et al., 2014). These authors show that gas emissions are remarkably intensive at the main ridge of the Forlandet moraine complex, and they postulate that they may be related to thawing permafrost.

Because of the warming potential of methane, there have been long-standing efforts to quantify how much of the methane discharged at seafloor seeps reaches the atmosphere. In addition, it is important to quantify the amount of methane that remains in the ocean, as aerobic microbial oxidation of methane releases protons and thus may play a role in ocean acidification (Biastoch et al., 2011). There is therefore, a significant interest to understand the interactions among ice, ocean, microbiology and climate and their sensitivity to both natural and anthropogenic change in Arctic regions. The hydrographic objectives of HE450 were to quantify the relative roles of various sources of methane offshore Svalbard, and extend the study to include the less studied region along the shelf from 71^{o} to 76^{o}N.

The sampling was guided by hydroacoustic observation of flare sites as well as previous data of methane seepage in the area (Sahling et al., 2014). Samples were analyzed for their methane concentration onboard, which guided the sampling strategy as the expedition progressed. Additional selected samples were collected for characterization of isotopic composition of methane-carbon and water-oxygen, as well as nutrients and barium. The isotopic composition of methane is used to identify the methane sources (biogenic vs. thermogenic); and in addition, these data may provide information on the degree of methane oxidation. The $\delta^{18}O$ of ocean water is a conservative tracer and meteoric water in high latitudes is highly depleted in ^{18}O, therefore this parameter aids in quantifying the degree of mixing of glacier water and river run-off with ocean water.

5.2 Methods

Water sampling

Hydrocasts were carried out using the ship-based SBE911plus (Sea-Bird Electronics, Inc.) CTD, which is comprised of two conductivity (SBE 4c) and temperature (SBE3 plus) sensors and one pressure sensor. The system was additionally equipped with dissolved oxygen (DO, SBE 43), fluorometer (WET Labs, Eco FL) and transmissometer (WET Labs, C-Star) probes. The underwater unit was attached to a SBE 32 carousel water sampler with 11x4L water sampling bottles (OceanTest Inc.), which were closed at selected depths during the upcast. The CTD/rosette system was lowered with 0.5 m s^{-1} in the upper to intermediate water column and 0.2 m s^{-1} in bottom waters, whereas heaving in-between the bottle firing procedure was conducted with 0.3 to 0.5 m s^{-1}.

Methane analyses in water samples

For analyses of methane in the water column we used the procedure described by Gepraegs et al. (2016), based on headspace extraction and analyses using off-axis integrated output spectroscopy (ICOS). Water samples from the Niskin bottles were collected in three 140 ml syringes outfitted with a valve. The syringes were flushed and filled with 100 ml of water, with no air bubbles. Two of the syringes were used for the analysis and one served as a spare. After equilibration of the samples to room temperature, 40 ml of Zero Air (synthetic air without methane) were added to the syringes, which were then shaken for 1.5 min. The 80 ml of headspace gas were collected in another syringe and injected into the Los Gatos research Greenhouse Gas Analyzer (GGA, followed by dilution with 60 ml of Zero Air to reach the 140 ml of gas in the chamber required for the instrument to operate.

Methane analyses in air

We took advantage of the GGA capability to measure air samples using a continuous flow mode. Air was collected from an intake located 5 meters above the sea surface and monitored using the slow mode at frequencies of either 10 or 100 seconds. The continuous monitoring was only conducted when weather conditions allowed and when the instrument was not being used for water sample analyses.

Extraction of dissolved gas from water samples

For preparation of dissolved gas for subsequent analysis (e.g. δ13C-CH4), 600 to 800 mL of selected water samples were transferred from the Niskin bottles into pre-evacuated 1 L gas tight glass bottles. The dissolved gas was prepared from the water samples by high-grade vacuum extraction (Lammers & Suess, 1994; Rehder et al., 1999; Schmitt et al., 1991) within a few hours of collection. The liberated gas was taken from the extraction system via a septum with gas-tight syringes and transferred into 20 ml serum glass vials pre-filled with saturated NaCl solution for storage and onshore analysis. In total, 113 gas samples were prepared from water samples collected during 28 CTD stations.

5.3 Results

Water masses in the study area

We used the water mass classification of Slubowska-Wodengen et al. (2007) and the CTD data from 37 vertical profiles collected along the HE450 survey to map the prevailing oceanographic conditions.

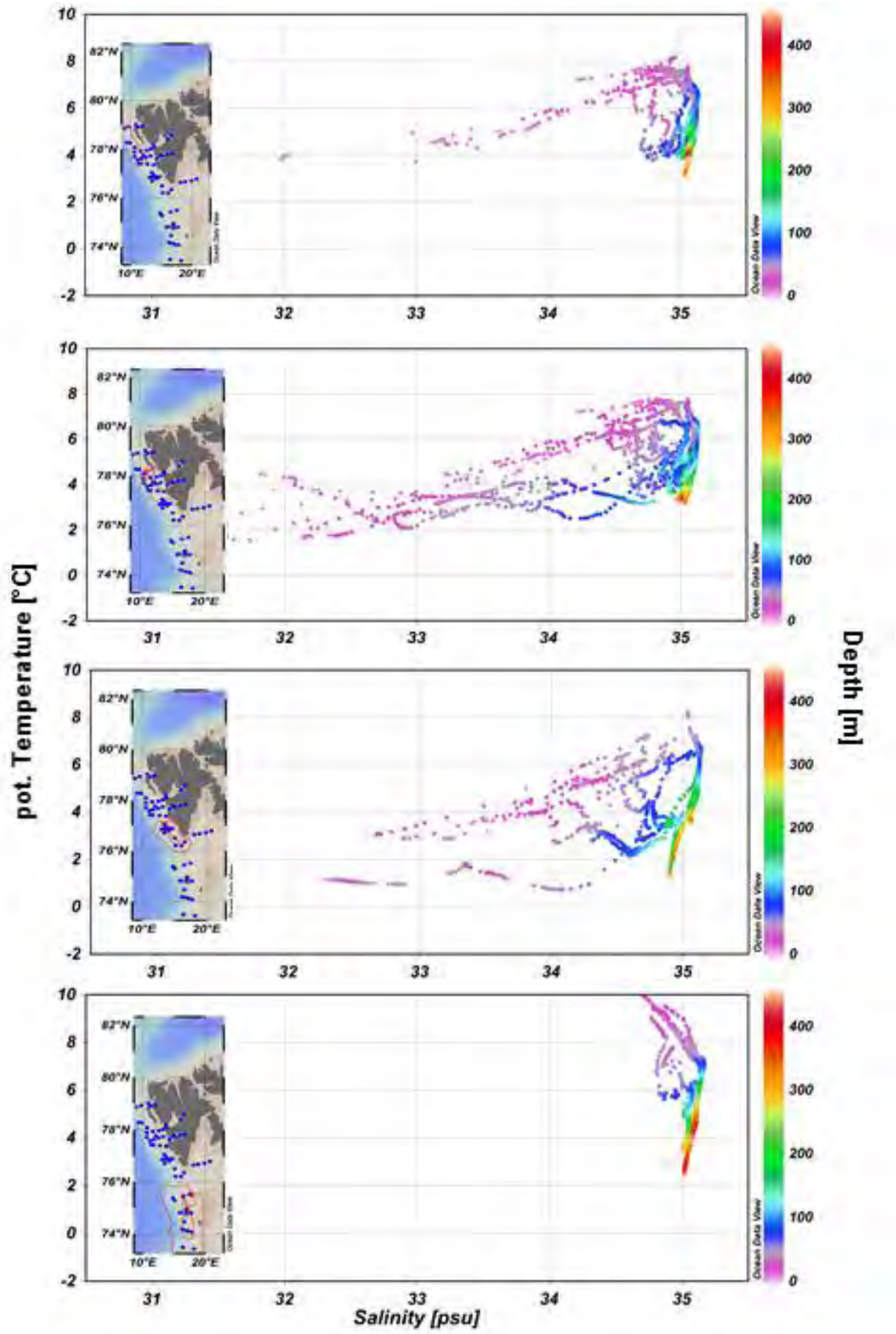

Fig. 19: TS diagrams of the study area. A) Barents Sea shelf/slope. B) Spitsbergen outer shelf. C) Spitsbergen inner shelf. D) Hornsund area.

In the surface layer, we observe the presence of two distinct water masses (Fig. 19). South of 75.5°N, the surface water is characterized by low salinity (34.7<S<34.9) and warm temperatures (5 to 10°C), which corresponds to Arctic Surface Water. Farther north along the Spitsbergen shelf, we observe a mixture of water masses that include the West Spitsbergen current (WSC) flows along the shelf break carrying Atlantic Water (T>2C and S>35) and a component of fresh Polar Water (PW), with low salinity (S<34.4) and colder temperatures (T<4°C), which is clearly distinct in the TS diagrams. Various mixtures of these surface water masses result in complex and variable TS diagrams. Underneath the surface fresh water pool the Atlantic Water (AW) is characterized by S>34.90 and T>3°C. The deepest water sampled, with S>34.9 and T<3°C corresponds to the Lower Arctic Intermediate Water (Slubowska-Wodengen et al., 2007).

Methane in the water column

The methane concentration in the 37 hydrocasts conducted during this cruise is illustrated in Figs. 20 to 22. We divide the stations in three general areas: Area 1, along the Barents shelf and slope (71° to 76°N); Area 2, Spitsbergen shelf and slope (76° to 79°N); and Area 3, Kongsfjorden.

Area 1. Barents Sea shelf (Fig. 20)

Water profiles for samples collected from 71° to 77°N are shown in Figure 20. From these hydrocasts, only CTD-3 was located directly over a flare area; CTD-29 was taken over a region of previously reported flares. These stations revealed concentrations in bottom water up to 50 nmol/l. In the other stations collected in water depths above 300 m in areas of no flare activity, we document elevated methane to maximum values of ~20 nmol/l. These results, tied to the observations of several flares in the area, indicate the presence of significant methane release in the sediments from several and perhaps abundant sites of micro-seepages distributed along the Barents shelf.

There is a marked concentration gradient between deep and surface waters, which is created by density stratification of the water masses. The elevated methane values are only found beneath water with σ_θ>27.75, in what is commonly referred to as transport along a pycnocline (Cynar and Yayanos, 1992). All values in shallow waters south of 76°N show background concentrations of <5nmol/l. The northernmost stations in the transect (CTD 26 and CTD 27), however show enrichment in surface waters to values of 18 and 9 nmol/l, respectively, consistent with other observations along the Spitsbergen shelf (section below).

It is worth noting that CTD-1, collected at 700 m water depth, only 7 km due west of station CTD-2, does not show the methane increase at depth observed in all stations along the shelf. The lack of horizontal extension of the methane plume is consistent with previous observations along Spitsbergen that document methane incorporated into bottom waters as it spreads northwards below the 27.75 pycnocline along the shelf and upper slope (Damm et al., 2005). The elevated methane values in the bottom water can be traced northwards along the Spitsbergen shelf and slope to Prins Karls Forland, as discussed in the section below.

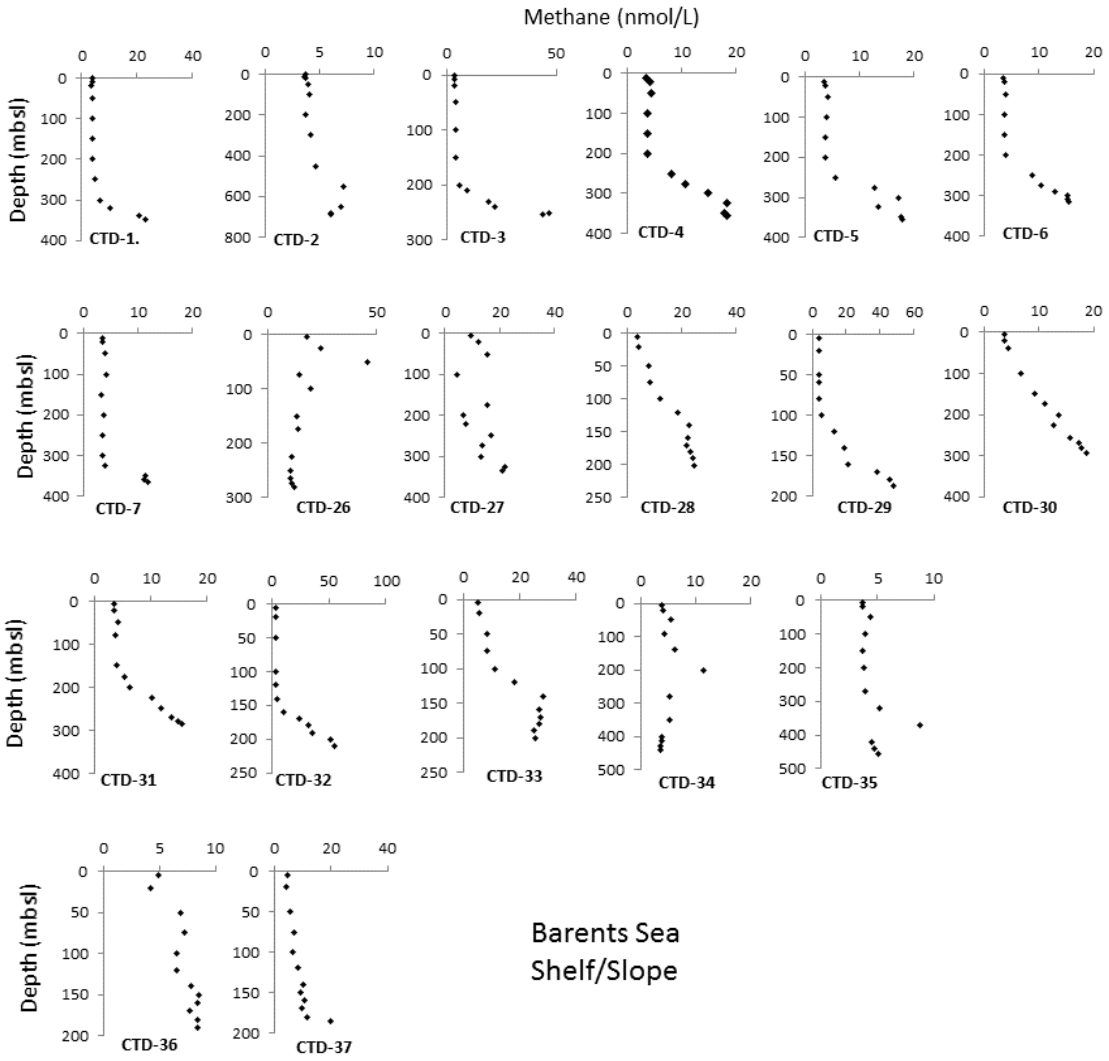

Fig. 20: Methane concentration profiles for stations along the Barents Sea shelf/slope (Area 1), for station locations see Figure 19.

Area 2, Spitsbergen shelf and slope region (Fig. 21)

There is intense flare activity and associated high levels of dissolved methane in the bottom waters of the shallow Spitsbergen shelf. The methane concentrations in the hydrocast stations collected along the inner shelf, all indicate bottom water enrichment, which at station CTD-8 reached values as high as 339 nmol/L. Some of these stations also have elevated values in near surface waters, ranging from 8 to 14 nmol/L, indicating that the Spitsbergen shelf may act as a methane source to the atmosphere.

The water column sampled north of Prins Karls Forland is characterized by the presence of two mid water maxima at ~70 and ~150 meters water depth. The 150 m mid-water maximum peak was observed in both stations CTD-13 and CTD 14, but more pronounced in CTD-13, with a maximum of 60 nmol/L. This likely corresponds to a methane plume originating at the mouth of Kongsfjorden, where intense flare activity was observed. The shallower mid-water maximum in CTD-15, with a methane content of 70 nmol/L at 50 m, likely reflects northwards transport of the shallow seeps off Prins Karls Forland (Sahling et al., 2014), which are located around 80 meters water depth. At station CTD-16, there is still a distinct increase above background between 75 and 100 m, but the methane

concentration is only 8 to 9 nmol/L. At this station there is also a slight increase towards depth, with a maximum of 17 nmol/L at 216 m water depth; which may reflect northwards transport of methane from the 200 m water depth seeps described by Sahling et al. (2014).

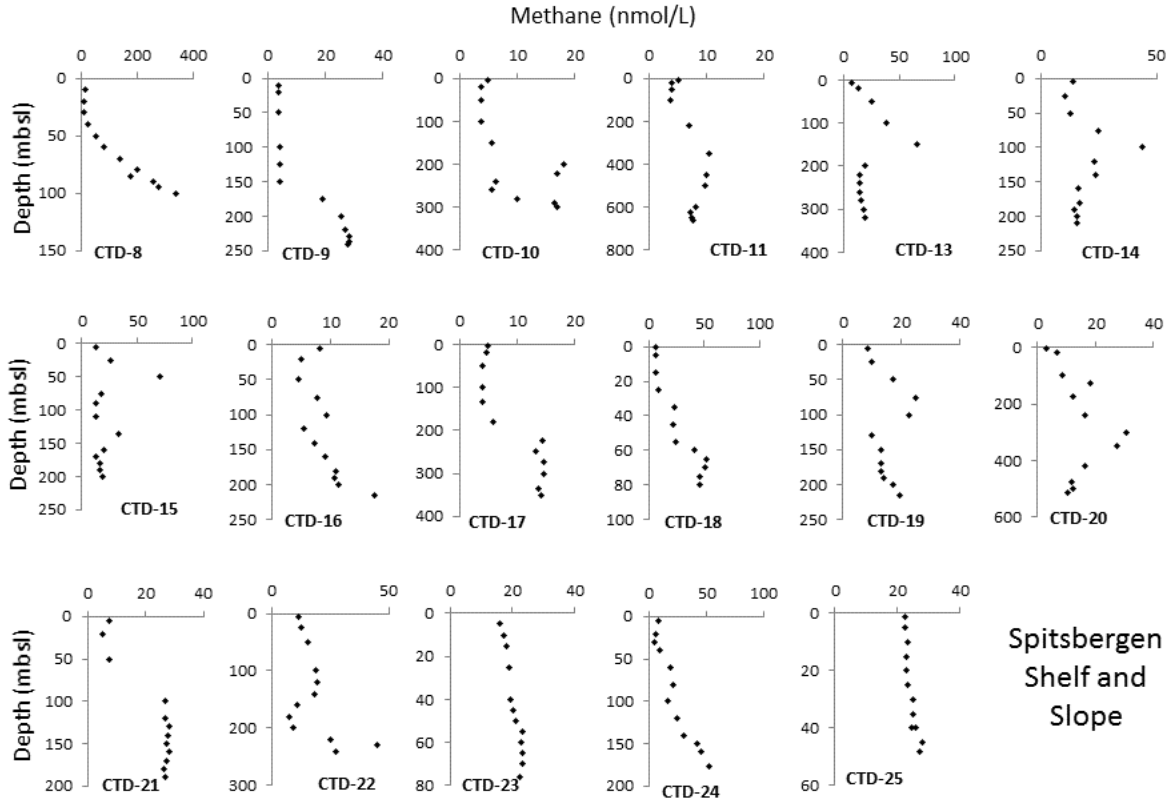

Fig. 21: Methane concentration profiles for stations along the Spitsbergen shelf/slope (Area 2), for station locations see Figure 19.

Area 3, Kongsfjorden (Fig. 22)

Only one CTD was collected within the fjord (CTD-12). The station was selected to sample the deepest waters of the fjord. At the onset of the hydrocast, there were no indications of flare activity at this location; however a flare was observed to appear during the hydrocast at ~150 m from our sampling location. Methane concentrations in this station are above 10 nmol/l throughout the water column, with a mid-water maximum of 20 nmol/l at 100 mbsl (Fig. 22).

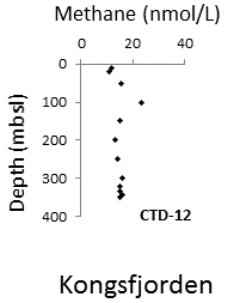

Fig. 22: Methane concentration profiles for station CTD-12 in Kongsfjorden, location shown in Figure 19.

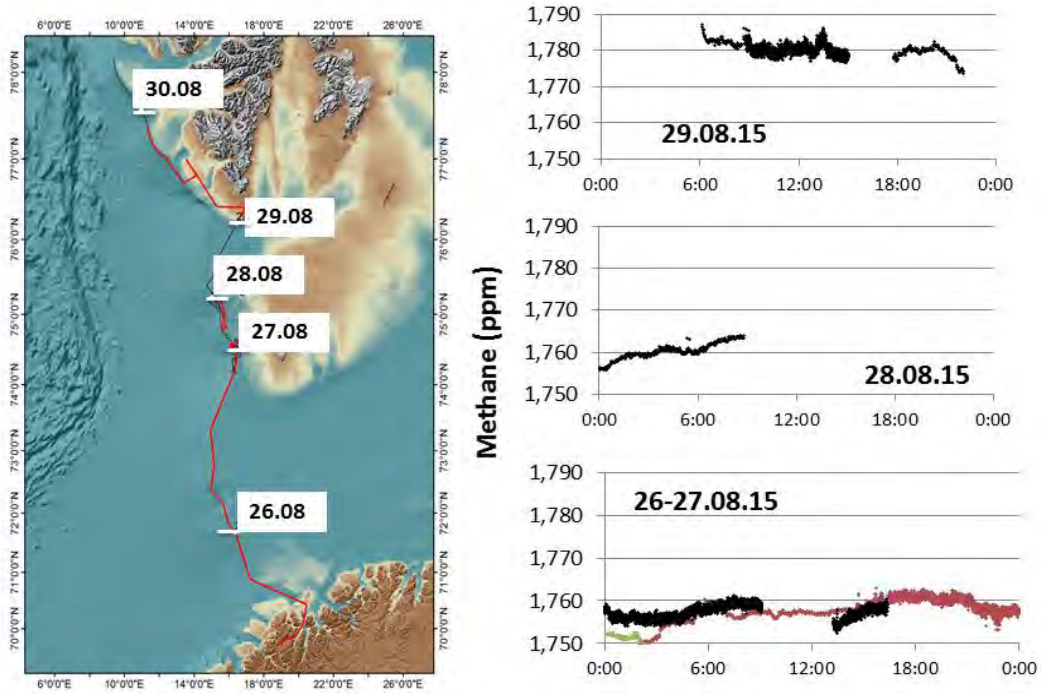

Fig. 23: Example of the methane in continuous air measurements, showing the data from 26.08.15 to 29.08.15 and the corresponding ship tracks.

Methane in air samples

Methane concentration in air samples is illustrated in Figure 23. Values for samples collected during the transit from Tromsø to Spitsbergen during 26.08. and 28.08., range from 1.7502 to 1.7619 ppm. In contrast, there is a marked increase in concentration along the shelf of Hornsund, with values ranging from 1.774 to 1.787 ppm, with maximum single-point measurements of up to 1.805 ppm (Fig. 23). These elevated values correspond to locations of active seepage along the shelf, where methane in the surface water ranges from 8 to 14 nmol/l, as measured in this study and in several other hydrocasts in this area collected during HE 449. The surface methane concentrations above saturation are confined to the shelf and do not extend towards the slope. Accordingly, air samples show a marked and rapid decrease from an average value of 1.78 ppm above the shelf seep region to the background concentration range of 1.750 to 1.762. Even above the active seepage areas offshore Prins Karls Forland, where numerous flares were observed during this cruise and by others (Westbrook et al., 2009; Gentz et al., 2013; Sahling et al., 2014), methane in air samples do not show significant elevation over background values. This is consistent with the observation that the dissolved methane plume remains below the pycnocline, with little vertical transport. Results from modeling and field work in this area and elsewhere have revealed that gas exchange between methane in bubbles and other gases in seawater is so rapid that just after a 20 m rise from the seafloor, only 20% of the initial methane remains in the bubble (Gentz et al., 2013).

5.4 Sound Velocity Profiles

(C.-W. Hsu, P. Wintersteller, M. Loher)

Applying the proper sound velocity profiles to multibeam system is necessary for controlling the quality of the data during the seafloor mapping. The values of sound velocity in water column depend on the pressure, density and temperature of water. Therefore, the sound velocities are varied with depth due to different water mass or the different physical property of each water depth.

During this cruise, the SVPs were calculated from pressure, salinity and temperature data from the CTD measurements. The data of each CTD cast were converted as .txt files then imported into excel sheet to calculate the sound velocities. The sound velocities were calculated by following the equation (1) (The UNESCO equation, Wong & Zhu (1995)).

In total 34 CTD casts were acquired during this cruise, and 34 SVPs were obtained after calculating by UNESCO. The range of sound velocity was between 1450 to 1490 m/s in the working area (Fig. 24). The SVPs where located near shelf edge of Svalbard showed similar pattern, the sound velocity increased as depth increase from near surface to 40 m, then velocity decreased from 40m to ~200 m reaching the minimum value of each profile, and velocity slightly increase again when depth increased. The SVPs in shelf edge of Kveithola trough also showed the similar pattern as upper part of shelf edge of Svalbard (< 200 m), the minimum value could be measured only at CTD-2 (Fig. 25).

According to the locations of CTD station, the SVPs in the west of Svalbard were grouped into four different areas. The profiles in Figure 26 indicated that significant difference could be found in the same area. Therefore, the proper sound velocity application should be done when bathymetric post-processing.

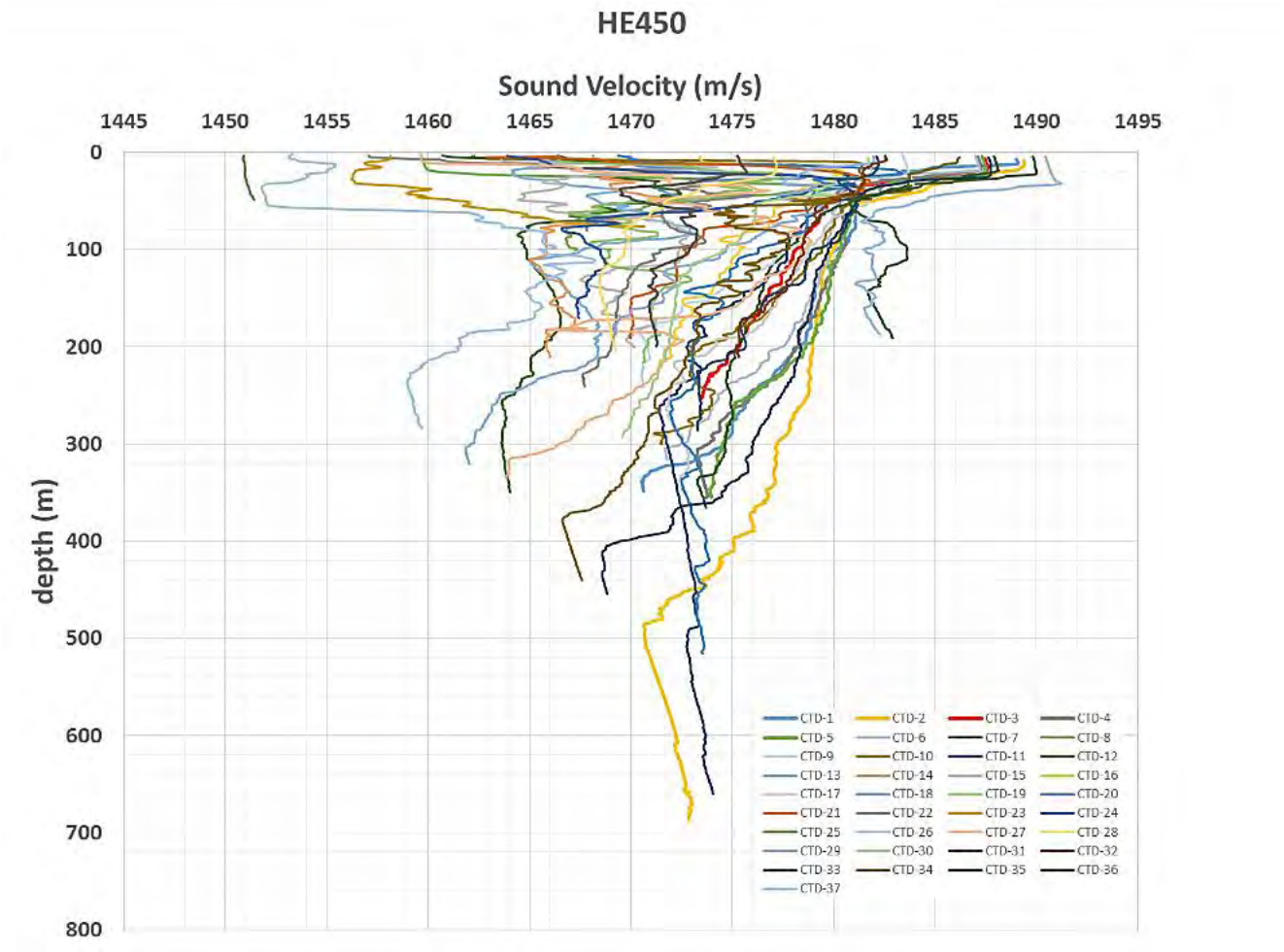

Fig.24: The sound velocity profiles of HE450. The sound velocity values were calculated from the CTD data (Pressure, salinity and temperature).

(a) (b)

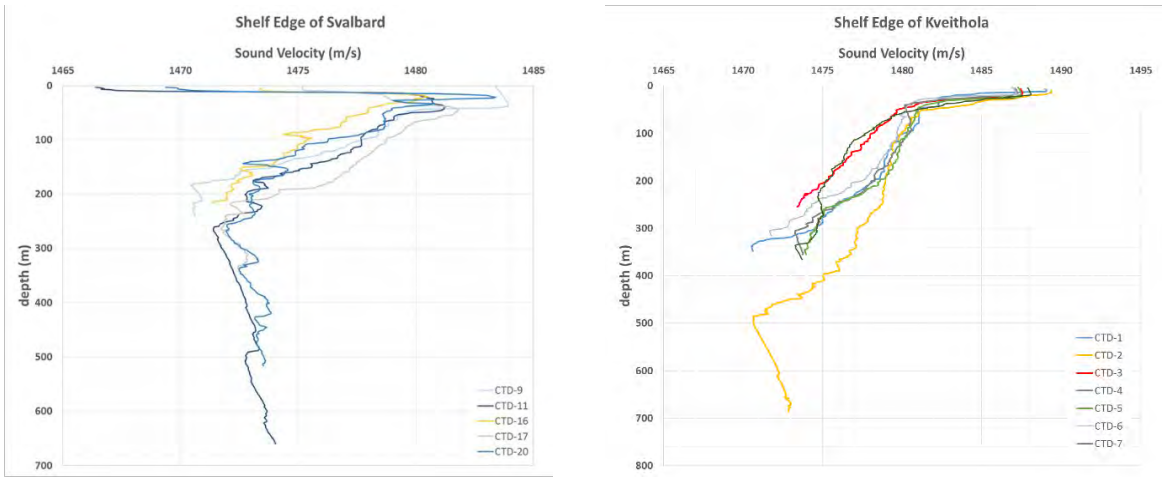

Fig. 25: The Sound Velocity Profiles of shelf edge showed the similar pattern in both area. In general, the vaule of sound velocity is higher in (b) than (a). This provided a very important information for applying proper sound velocity to post-processing the bathymetric data.

(a) (b)

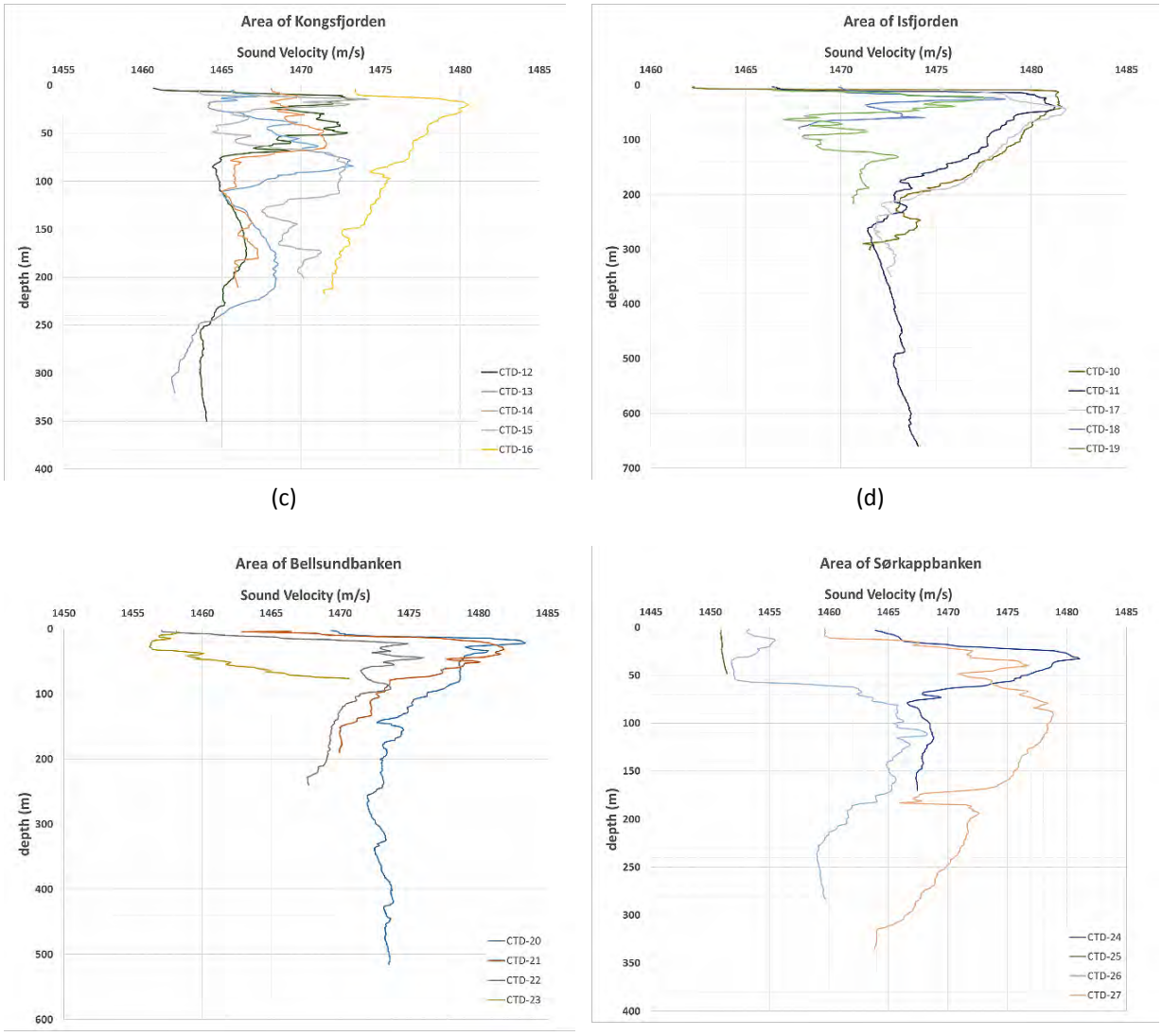

(c) (d)

Fig. 26: The sound velocity profiles in each area. The order (a to d) of figures are from north to south. For the detailed location of each station showed in chapter 3 (Figs. 7, 8, 10).

6 Sediment Sampling and Composition

(M. Loher)

6.1 Introduction and Sampling Techniques

Throughout the cruise a total of four sediment grab samplers, two gravity cores and two mini-corers successfully recovered seafloor material (s. map insets on Fig. 27 and Fig. 28 for locations). The grab samples were collected with a small “Backengreifer” (BG) usually with the aim of investigating the seafloor prior to the deployment of a gravity core. Mini-cores (MICs) were collected to sub-sample sedimentary material for geochemical analyses. For gravity cores (GCs), an overburden-weight of about 1100 kg was attached and plastic bags were used instead of liners in order to guarantee quick access to the recovered material. Due a mechanical defect in the winch as well as slacking and twisting of the winch-cable, no more than two GCs could be deployed. Safety reasons demanded the abandonment of any further gravity coring attempts after GC-2.

Sedimentological investigations focused on two general sampling areas: the Isfjordbanken Margin (Fig. 27) and the Kongsfjorden (Fig. 28). The specific sites were chosen where gas flares had previously been hydroacoustically detected in the watercolumn and traced to their emission sites on the seafloor.

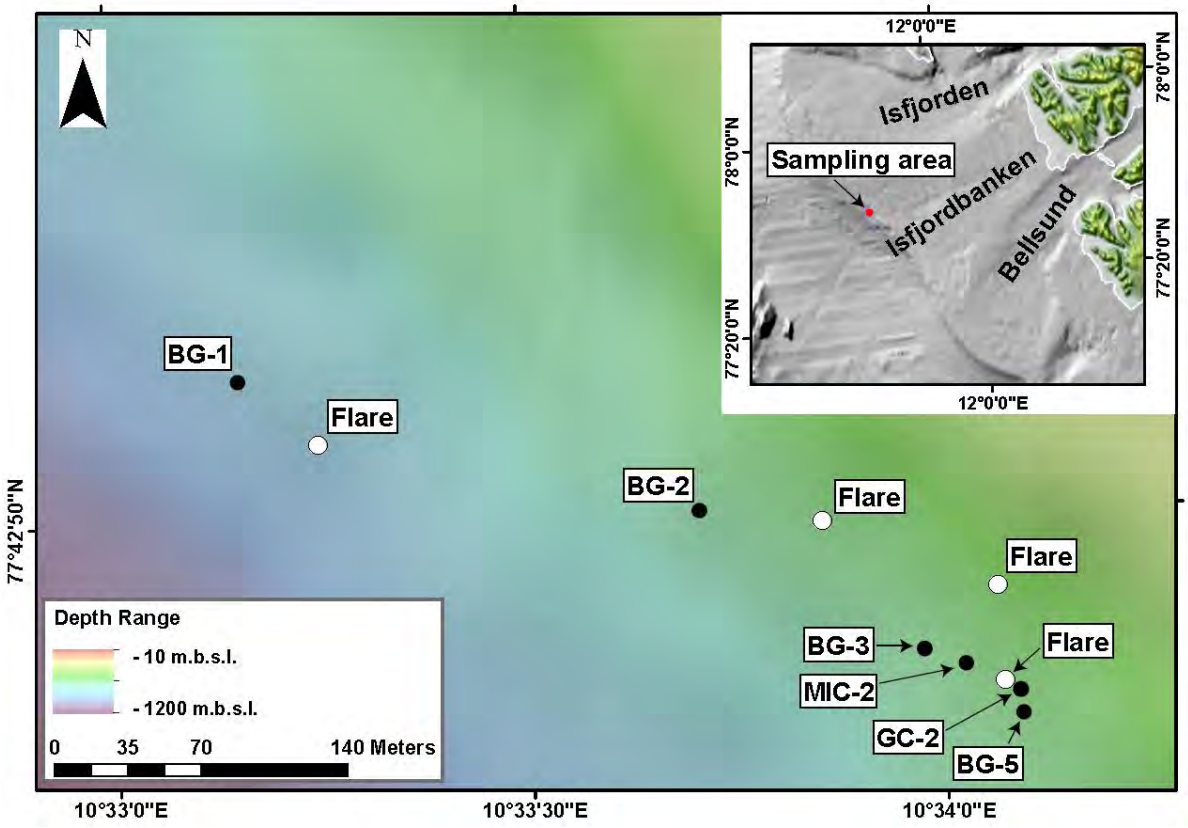

Fig. 27: Multibeam bathymetry map of the Isfjordbanken Margin sampling area with sediment sampling stations and flare sites; BG = grab sample, MIC = mini-cores, GC = gravity core.

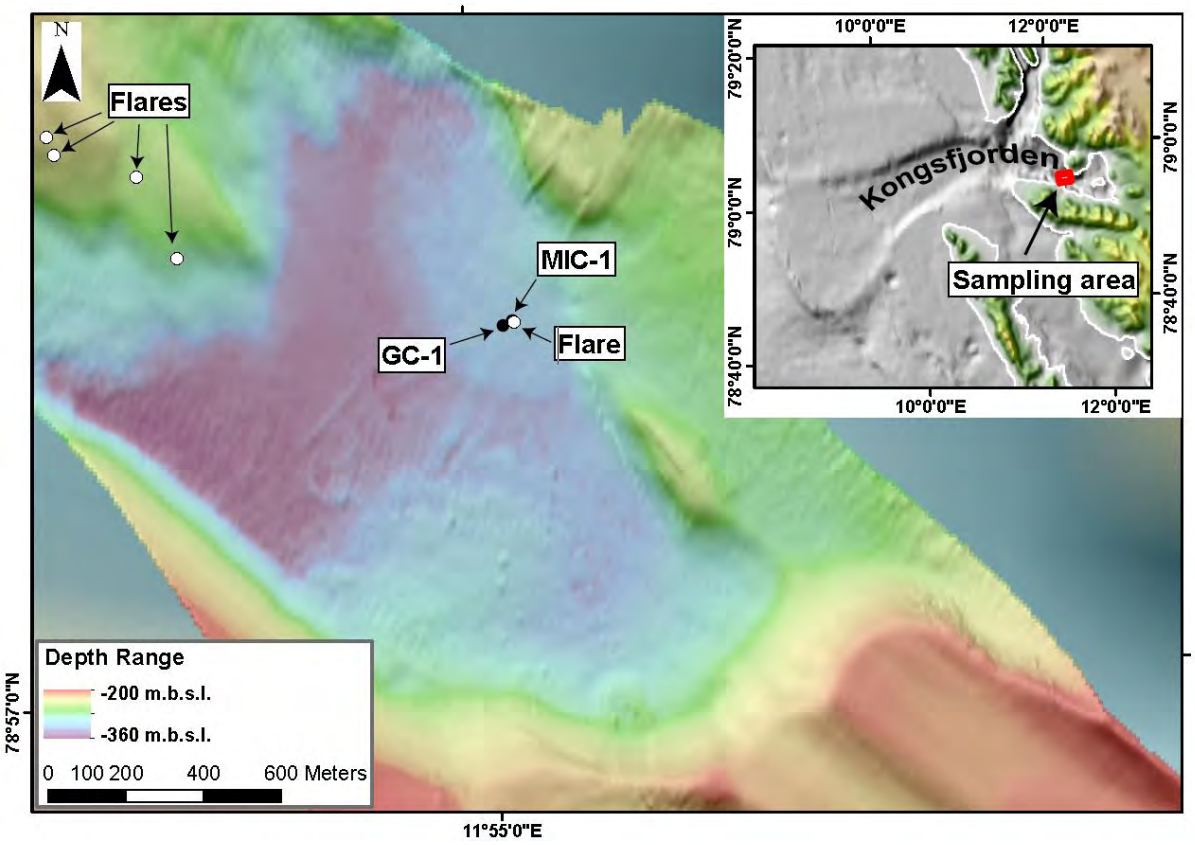

Fig. 28: Multibeam bathymetry map of the Kongsfjorden sampling area with sediment sampling stations and flare sites; BG = grab sample, MIC = mini-cores, GC = gravity core.

Recovered sediments were macroscopically described (Munsell color chart, HCl reaction, grain composition, structures, etc.). Where present, gravel samples were sieved and washed in order to describe their principal contents and provide selected source-rock information. Washed samples from the GC, BG and MIC were stored in plastic bags, but apart from the sub-sampled sediment no GC-sections were stored.

6.2 Sediment Composition

Isfjordbanken Margin (BG-1, 2, 3, 5, MIC-2, GC-2)

For the detailed core and sample descriptions the reader is referred to Appendix 2. Geological details about the Isfjorden area as well as other information has been taken from the Geoscience Atlas of Svalbard by Winfried K. Dallmann (Norsk Polarinstitutt, 2015).

This sampling location is situated at the outer part of the shelf (at the shelf break) where flares had been hydroacoustically detected in the watercolumn (Fig. 27). The Isfjordbanken is an area where the erosive processes of past glacial ice was reduced (in opposition to the glacial troughs) and therefore has a smooth and sub-horizontal morphology. Sedimentation at this location is mainly influenced by glacio-marine processes today but in the past experienced the deposition of large amounts of sediments at the margin of ice-streams (the grounding zone wedge and trough mouth fan).

Table 4: Overview table of sediment samples during HE450.

Date	GeoB-Nr.	Station Name	Area/Site/Target	Short sediment description
30/08/2015	20212-1	BG-1	Isfjordbanken Margin (seep site)	Poorly sorted, grain supported gravelly sand with a silty-clay matrix; no HCl reaction;
31/08/2015	20214-1	MIC-1	Kongsfjorden	11.5 cm, brownish red clayey silt.
31/08/2015	20214-2	GC-1	Kongsfjorden	360 cm recovery; finely laminated silty clay, gravel interval, homogeneous black and reddish brown clays
02/09/2015	20219-1	BG-2	Isfjordbanken Margin	Poorly sorted gravelly sand with a silty matrix.
02/09/2015	20220-1	BG-3	Isfjordbanken Margin (seep site)	Poorly sorted, sandy gravel (possibly covering the immediate seafloor) with predominantly silty material as a matrix / down below.
02/09/2015	20220-2	BG-4	Isfjordbanken Margin (seep site)	Empty, failed release
02/09/2015	20220-3	BG-5	Isfjordbanken Margin (seep site)	Poorly sorted, sandy gravel with a silty to sandy matrix.
02/09/2015	20220-4	GC-2	Isfjordbanken Margin (seep site)	190 cm recovery; homogeneous dark greenish gray, sandy silt (no HCl reaction), with abundant, rounded (smoothed but abraded and scraped pebbles (mm to pluri-cm). Most probably ice rafted debris and/or dropstones.
02/09/2015	20222-1	MIC-2	Isfjordbanken Margin (seep site)	5 cm in only one liner; silty clay with cm-sized pebbles

The first grab sample (BG-1) was collected on 30 August under unfavorable weather conditions and the exact target (a gas bubble emission site) was probably not sampled. Sand and gravel material in a silty matrix was retrieved.

The cruise re-visited this area on 2 September in order to collect further grab samples and a gravity core as well as mini-cores. Different gas bubble emission sites had been picked on the seafloor as the desired targets but the vessel positioning was never exact enough to precisely deploy the tools (Fig. 27). The grab samples (BG-2, 3, 5) contained similar material to BG-1. From BG-3 it seemed that larger gravels (up to 15 cm diameter, Fig. 29A) were overlying softer (clayey silt) sediments below. The successful recovery of a 1.9 m sediment core revealed that the sediments are composed of a dark, greenish gray, homogeneous silty sediment. Only one interval (98 – 109 cm, Fig. 29B) showed a discoloration of a more yellowish tint. Throughout the core, poorly sorted gravel particles were abundantly dispersed (Fig. 29C). None of the collected sediment samples contained any indication of an active seep site but non-seep related biogenic components were found in all BGs (Fig. 29D, E, F).

Fig. 29A: Heterogeneous sediment composition of sieved BG-3 material; the largest gravel (yellowish brown, on left) is of magmatic origin and the light gray (top) is a sandstone showing a strong reaction with 10% HCl.

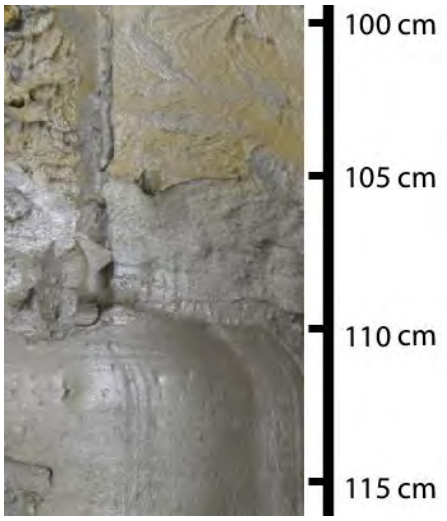

Fig. 29B: GC-2 core section showing the transition from a yellow tinted facies to the homogeneous, dark greenish gray silt with pebbles / dropstones below.

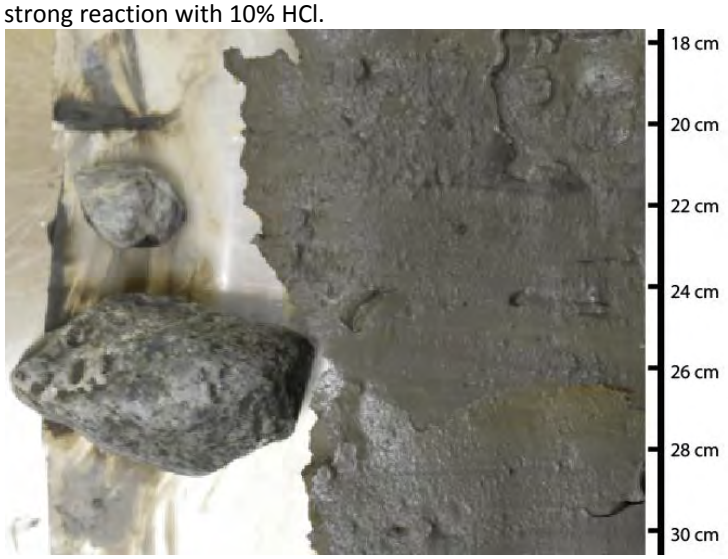

Fig. 29C: Rounded and smoothed dropstones are found abundantly throughout the whole GC-2.

Fig. 29D: Brittle star attached to a pebble, recovered by BG-5; the size is about 3 cm.

Fig. 29E: Sea urching (ca. 1.5 cm diameter) recovered in BG-5.

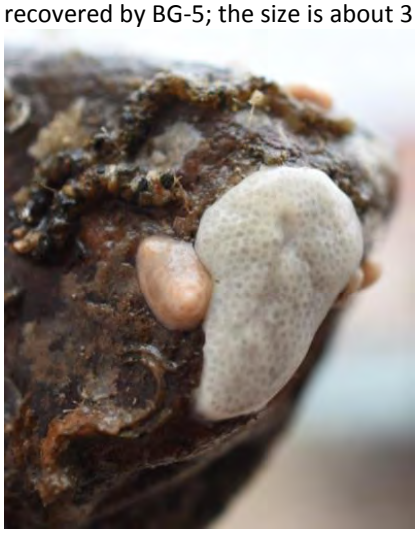

Fig. 29F: Sponge (ca. 3 cm) encrusting a large pebble recovered in BG-5.

For the detailed core and sample descriptions the reader is referred to Appendix 2. Geological details about the Kongsfjorden area as well as other information has been taken from the Geoscience Atlas of Svalbard by Winfried K. Dallmann (Norsk Polarinstitutt, 2015).

With regard to the many valley glaciers around the Kongsfjorden area a significant amount of sediment supply is guaranteed through direct (glacial melt-out, iceberg rafted debris, dropstones) or indirect (seasonal meltwater input) glacial processes in addition to rockfalls and debris flows from the fjord flanks as well as through glacially- or non-glacially-fed rivers. Furthermore, the absence of a sill at the mouth of the Kongsfjorden allows warmer Atlantic water to enter the fjord relatively unhindered, influencing the seasonal water composition.

The MIC-1 core only contained 11.5 cm of sediment composed of a brownish red clayey silt. This is similar to the topmost of the five sedimentary facies found in GC-1, which shows a clear lamination of up to three colors: brownish red, greenish gray and dark brown, consisting of silty clay (Fig. 30A). Below 127 cm the laminations give way to a greenish gray, patchy clay with silt. At 245 cm the sediment gradually transitions to a more sandy facies and finally to a sandy gravel interval. From 280 cm on follows a homogeneous clay with abundant (silt sized) foraminifera. A 10 cm interval of a very dark/black clay occurs from 322 cm and is replaced by a homogeneous reddish gray clay from 332 cm to the base of the core. Sub-rounded but scraped and abraded pebbles can be found throughout the core and probably represent dropstones transported by calved icebergs.

The laminated core interval represents different sedimentological or geochemical processes occurring at periodic intervals (e.g. yearly). While entering the Kongsfjorden, icebergs were constantly being rafted seawards, some of them loaded with a reddish brown sediment, similar to what has been observed in the cores (Fig. 30B). Outcrops of red sandstone and shales were later observed near the tongue of the Kronebreen glacier mouth and probably provides the source material (Fig. 30C). Further, it is known that after the sea-ice breakup (spring time) biological productivity is enhanced, leading to an increased flux of organic matter to the seafloor (this could explain the greenish, probably organic rich laminae). In addition, meltwater runoff and glacier base runoff increases during summer and is very low during winter. These processes cause strong plumes of suspended sediment, the concentration of which decreases, as the runoff water mixes with the seawater the further away from the glacial front it flows.

The deeper sediment facies of GC-1 clearly contain a high clay content (of glacial origin?) and foraminifera indicating that also marine sediments are being accumulated.

The gravel interval in GC-1 seems to represent a relatively short period of time when much coarser material got deposited at the coring location. This may have resulted from mass wasting close to the glacier front. Further, the bathymetric data reveals flutes and esker-like structures visible on the seafloor close to the coring site, which are also composed of coarse grained, glaciogenic materials.

The homogeneous clay at the deepest part of GC-1 could represent material from turbid waters, discharged off the glacial fronts and the variability in color may result from changes in the source material.

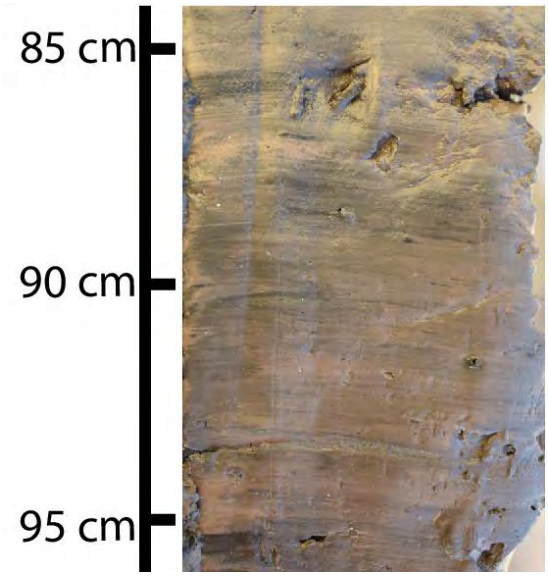

Fig. 30A: Laminated facies in GC-1; note the reddish brown color similar to the sediment on the iceberg of Fig. 30B)

Fig. 30B: Sediment loaden, turned over, iceberg rafting seawards in the Kongsfjorden.

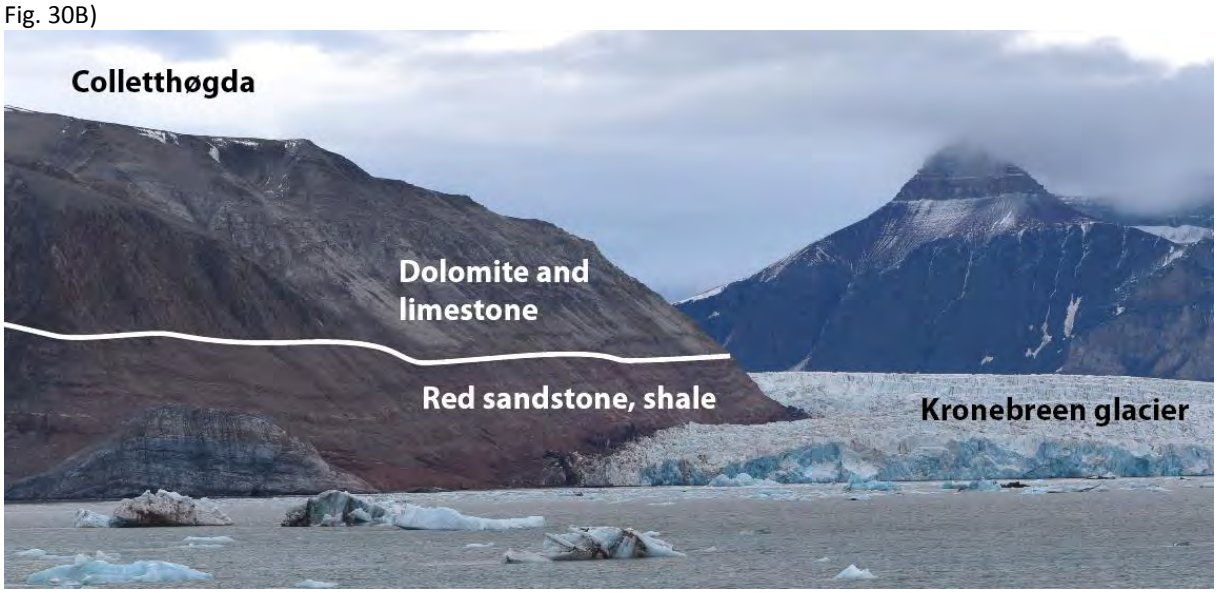

Fig. 30C: At the base of the Colletthøgda the red sandstone and shales are supplied to the Kronebreen glacier which calves sediment laden icebergs into the Kongsfjorden. Some of the sediments are then rained out or dumped on the seafloor when the iceberg melts or turns over during its passage.

7 Geochemistry of Pore Water

(W.-L. Hong, H. Yao, T. Pape)

7.1 Introduction and Motivation

Pore fluid geochemistry provides essential information about fluid sources and flow. By analyzing the concentration and isotopic composition of target species in the pore fluid, we are able to both identify the biogeochemical processes and quantitatively estimate the fluxes of key solutes from sub-bottom to seafloor. During HE450 cruise, two gravity cores and one mini core were recovered from Kongsfjorden and the continental margin area west of Spitsbergen (for locations see Figure 10). We conducted pore water sampling and analyzed time-sensitive items on board. We also sampled sediments for potential microbiology and biomarker characterization as well as shorebased micropaleontology investigations. In Table 5 we summarize the number of samples and analyses done on these three cores.

Table 5: Summary of geochemical samples.

	Length (cm)	Alk	Fe^{2+}	SO_4	HS / $\delta^{34}S$	$\delta^{13}C$	Nutrient	Cations	Sed. Geochem	Biomarker /foram	Micro -bio	Dissolved CH_4
GeoB20214-1 MIC-1	11.5	3		3	3	3	3	3	7		0	0
GeoB20214-2 GC-1	350	10	16	16	10	9	10	16	19	17		12
GeoB20220-4 GC-2	180	9	18	18	0	0	0	16	34	0	5	9

7.2 Method

In Figure 31 we summarize the porewater sampling protocol. We not always had enough pore water for all subsampling. The porewater for onboard analyses, sulfate and cation concentration offshore have the highest priority and aliquots for these analyses were taken from all samples.

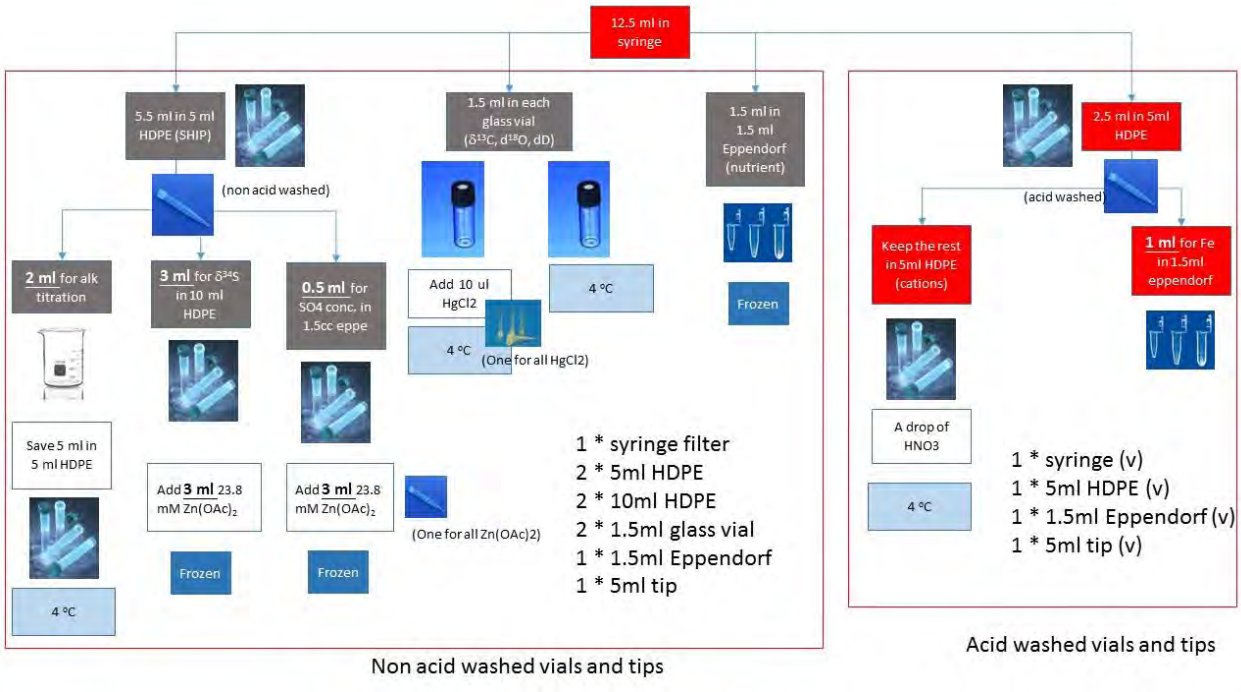

Fig. 31: Summary of porewater sampling protocol during HE450.

Alkalinity titration

Total alkalinity was determined with a pH-controlled titration to a pH just under 4 using a Metrohm 917 Ti-Touch titrator, within 3 hours from core recovery. The pH electrode was calibrated against pH 4, 7 and 10 Metrohm Instrument buffers. We used 12M reagent grade HCl (Sigma-Aldrich Prod. #: 84415) diluted with MilliQ water to 0.012M, which was calibrated on a daily basis by titrating a reference seawater sample and a 0.01M Borax standard. Samples (2ml) were diluted with 15 ml of 0.7M KCl solution before titration. The amount of acid and pH was manually recorded during each addition. Alkalinity was calculated from the Gran function plots using 8 to 10 points from pH 4.7 to 3.9. From the repeated measurements of standards (n=7), the uncertainty is around 1.

Fe^{2+} concentration through spectrophotometric method

We measured the concentration of dissolved Fe^{+2} by spectrophotometric method with Shimadzu UV1280 spectrophotometer under wavelength 565 nm. We weighed all chemicals (iron sulfate heptahydrate, ascorbic acid, and Ferrospectral) needed onshore and preserved them in dark containers. To make standard solutions and color complexation reagent, we prepared anoxic 0.7M KCl solution and MilliQ water onshore. This was done by autoclaving KCl solution and MilliQ water under 121°C for 20 minutes. We bubbled them with N_2 gas for 15 minutes before the temperature drops to room temperature. The anoxic solution was extracted onboard by applying a positive N_2 atmosphere. For the calibration curve, we made 10 calibration points with 1.1 to 16.7 μM $FeSO_4 \cdot 7H_2O$ standards (Sigma-Aldrich prod. #: 215422) and 2 background check with our anoxic MilliQ and KCl solution. This was done daily before measuring our porewater samples. After adding 50 μl of 9.72 mM Ferrospectral solution (Merck prod. #: 111613) in each 1 ml of pore water sample, the samples vials were stored in dark for 5-10 minutes to complete the reaction. Proper dilution of samples was made before adding Ferrospectral solution.

Concentrations of methane dissolved in pore water

For vertical profiling of methane concentrations in both gravity cores the headspace technique was used. 3 ml of sediment were taken with cut-off syringes at defined depths (20 to 25 cm resolution) and transferred into 20 ml glass vials prefilled with 5 ml of 1 M NaOH. For establishing equilibrium between the dissolved gas and the headspace gas the samples were shaken with an orbital shaker for 2 hours and left for further 24 hours. The headspace gas was analyzed for methane concentrations by gas chromatography (Pape et al., 2010).

7.3 Preliminary Results

In Figure 32 we present the preliminary results of onboard analyses of total alkalinity and Fe^{2+} concentration in the porewater. We combine the results from the two cores in Kongsfjorden (GeoB20214-1&-2) as they were taken from almost the same location. At this site, Fe^{2+} concentration drops to background level at *ca.* 15 cmbsf and marks the end of iron reduction zone. Alkalinity gradually increases below such depth until 2.4 mbsf. We did not have enough water for titration for the last three samples. However, based on the profile obtained onboard, alkalinity may have reached *ca.* 20 mM at the bottom of the core (3 mbsf), indicating that we have not penetrated the sulfate reduction zone.

Concentrations of methane in the headspace gas from core GeoB20214-2 were generally low (<4µM) if compared to those in samples from methane-rich sediments in other regions. However, a trend of increasing methane concentrations with increasing depths indicates slight methane upward migration at this site.

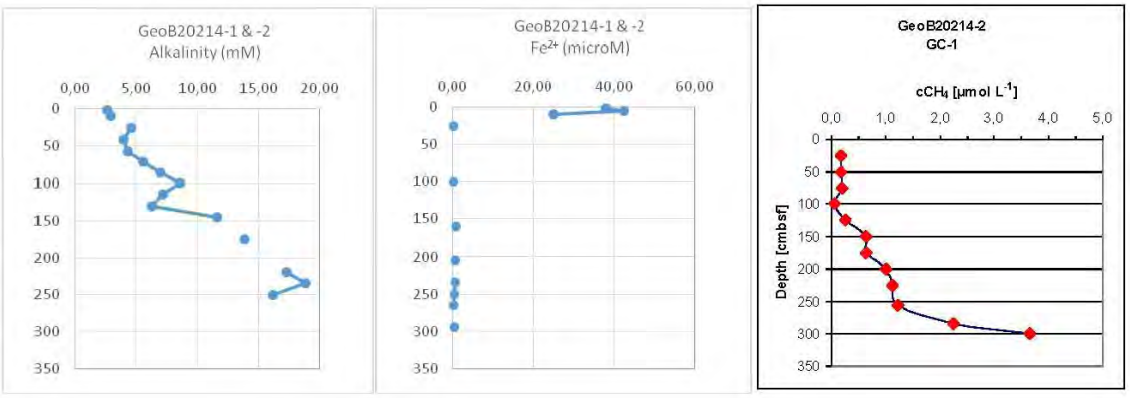

Fig. 32: Preliminary results of alkalinity, Fe^{2+} concentrations (in pore water) and CH_4 concentrations (in headspace gas) obtained for cores GeoB20214-1 (MIC-1) and GeoB20214-2 (GC-1) taken in the Kongsfjord.

For the gravity core taken from Spitsbergen continental margin (GeoB20220-4; GC-2 at the Isfjordenbanken Margin), Fe^{2+} concentration is higher than 50 µM in all except for the first four samples, suggesting the almost two meters long sediment core recovered is still within iron reduction zone (Fig. 33). Alkalinity is close to seawater values (2.8 to 3 mM) throughout the core, reflecting no signal from deeper fluid. The same conclusion can be drawn from the methane concentration profile that indicates comparably low methane concentrations (<1.5µM) throughout the core.

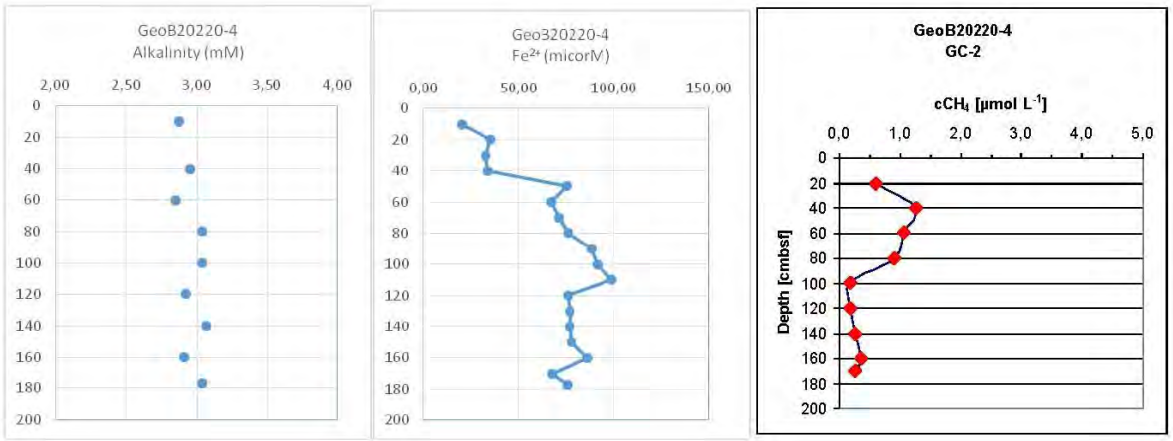

Fig. 33: Preliminary results of alkalinity, Fe^{2+} concentrations (in pore water) and CH_4 concentrations (in headspace gas) obtained for core GeoB20220-4 (GC-2) taken at the Isfjordbanken Margin.

8 References

Archer, D. and Buffett, B. (2005) Time-dependent response of the global ocean clathrate reservoir to climate and anthropogenic forcing, Geochem. Geophys. Geosys., 6, Q03002.

Berndt, C., Feseker, T., Treude, T., Krastel, S., Liebetrau, V., Niemann, H., Bertics, V. J., Dumke, I., Dünnbier, K., Ferré, B.,Graves, C., Gross, F., Hissmann, K., Hühnerbach, V., Krause, S.,Lieser, K., Schauer, J., and Steinle, L. (2014) Temporal constraints on hydrate-controlled methane seepage off Svalbard, Science, 343: 284–287.

Biastoch, A., Treude, T., Rüpke, L.H., Riebesell, U., Roth, C., Burwicz, E.B., Park, W., Böning, C.W., Latif, M., Madec, G. and Wallmann, K. (2011) Rising Arctic Ocean temperatures cause gas hydratedestabilization and ocean acidification, Geophysical Research Letters, 38, L08602.

Caress, D.W. and Chayes, D. N. (1995). New Software for Processing Sidescan Data from Sidescan-Capable Multibeam Sonars. IEEE Oceans '95, San Diego, CA., IEEE.

Chabert, A., Minshull, T.A., Westbrook, G.K., Berndt, C., Thatcher, K.E., and Sarkar, S. (2011) Characterization of a stratigraphically constrained gas hydrate system along the western continental margin of Svalbard from ocean bottom seismometer data, J. Geophys. Res., 116, B12102.

Chand, S., Thorsnes, T., Rise, L., Brunstad, H., Stoddart, D., Bøe, R., Lågstad, P., Svolsbru, T. (2012) Multiple episodes of fluid flow in the SW Barents Sea (Loppa High) evidenced by gas flares, pockmarks and gas hydrate accumulation. Earth and Planetary Science Letters 331–332: 305-314.

Cynar, F.J., Yayanos, A.A. (1992) The distribution of methane in the upper waters of the southern California Bight. Journal of Geophysical Research: Oceans 97: 11269-11285.

Dallmann, W.K. (ed.) (2015) Geoscience Atlas of Svalbard. Norwegian Polar Institute Report Series 148. Tromsø, Norway: Norwegian Polar Institute.

Damm, E., Mackensen, A., Budéus, G., Faber, E., and Hanfland, C. (2005) Pathways of methane in seawater: Plume spreading in an Arctic shelf environment (SW Spitsbergen), Cont. Shelf Res., 25: 1453-1472.

Fisher, R.E., Sriskantharajah, S., Lowry, D., Lanoisellé, M., Fowler, C.M.R., James, R.H., Hermansen, O., Lund Myhre, C., Stohl, A., Greinert, J., Nisbet-Jones, P.B.R., Mienert, J., and Nisbet, E.G. (2011) Arctic methane sources: Isotopic evidence for atmospheric inputs, Geophys. Res. Lett., 38: L21803.

Freudenthal, T. and Wefer, G. (2013) Drilling cores on the sea floor with the remote-controlled sea floor drilling rig MeBo. Geoscientific Instrumentation, Methods and Data Systems, 2(2): 329-337.

Gentz, T., Damm, E., Schneider von Deimling, J., Mau, S., McGinnis, D. F., and Schlüter, M. (2013) A water column study of methane around gas flares located at the West Spitsbergen continental margin, Continental Shelf Research 72: 107–118.

Gepraegs, P., Torres, M.E., Mau, S., Kasten, S., Roemer, M., Bohrmann, G. (2016) Carbon cycling fed by methane seepage at the shallow Cumberland Bay, South Georgia, sub-Antarctic. Geochem. Geophys. Geosyst. 17, accepted.

Ker, S., Le Gonidec, Y., Marsset, B., Westbrook, G.K., Gibert, D., Minshull, T.A. (2014) Fine-scale gas distribution in marine sediments assessed from deep-towed seismic data. Geophysical Journal International 196 (3): 1466-1470

Knies, J., Damm, E., Gutt, J., Mann, U., and Pimnturier, L. (2004) Nearsurface hydrocarbon anomalies in shelf sediments off Spitsbergen: Evidence for past seepages, Geoch., Geophys., Geosyst., 5: 14 p.

Lammers, S. and Suess, E. (1994) An improved head-space analysis method for methane in seawater, Mar. Chem., 47: 115-125.

Landvik, J.Y., Ingólfsson, Ó., Mienert, J., Lehman, S.J., Solheim, A., Elverhøi, A., Ottesen, D.A.G. (2005) Rethinking Late Weichselian ice-sheet dynamics in coastal NW Svalbard. Boreas 34: 7-24.

Mienert, J., Vanneste, M., Haflidason, H., and Bünz, S. (2010) Norwegian margin outer shelf cracking:a consequence of climate-induced gas hydrate dissociation? International Journal for Earth Sciences 99, Supplement 1: 207–225

Ó Cofaigh, C., Larter, R.D., Dowdeswell, J.A., Hillenbrand, C.D., Pudsey, C.J., Evans, J., Morris, P. (2005) Flow of the West Antarctic Ice Sheet on the continental margin of the Bellingshausen Sea at the Last Glacial Maximum. Journal of Geophysical Research: Solid Earth 110: B11.

Ostanin, I., Anka, Z., di Primio, R., Bernal, A. (2013) Hydrocarbon plumbing systems above the Snøhvit gas field: Structural control and implications for thermogenic methane leakage in the Hammerfest Basin, SW Barents Sea. Marine and Petroleum Geology 43: 127-146.

Pape, T., Bahr, A., Rethemeyer, J., Kessler, J.D., Sahling, H., Hinrichs, K.-U., Klapp, S.A., Reeburgh, W.S., Bohrmann, G. (2010) Molecular and isotopic partitioning of low-molecular-weight hydrocarbons during migration and gas hydrate precipitation in deposits of a high-flux seepage site. Chemical Geology 269: 350-363.

Rajan, A., Mienert, J., and Bünz, S. (2012) Acoustic evidence for a gas migration and release system in Arctic glaciated continental margins offshore NW-Svalbard, Mar Petrol Geol 32: 36-49.

Rebesco, M., Özmaral, A., Urgeles, R., Accettella, D., Lucchi, R.G., Rüther, D., Winsborrow, M., Llopart, J., Caburlotto, A., Lantzsch, H., Hanebuth, T.J.J. (online 2016) Evolution of a high-latitude sediment drift inside a glacially-carved trough based on high-resolution seismic stratigraphy (Kveithola, NW Barents Sea). Quaternary Science Reviews, in press, corrected proof.

Rehder, G. (1999) Quellen und Senken marinen Methans zwischen Schelf und offenem Ozean, GEOMAR, Kiel, 161 pp.

Ritzmann, O., Jokat, W., Czuba, W., Guterch, A., Mjelde, R., Nishimura, Y. (2004) A deep seismic transect from Hovgård Ridge to northwestern Svalbard across the continental-ocean transition: A sheared margin study. Geophysical Journal International 157: 683-702.

Sahling, H., Bergès, B., Boelmann, J., Dimmler, W., Geprägs, P., Glockzin, M., Kaboth, S., Nowald, N., Pape, T., Römer, M., Dos Santos Ferreira, C., Schroedter, L., Tomczyk, M. (2012) R/V Heincke cruise report HE387. Gas emissions at the Svalbard continental margin. Longyearbyen - Bremerhaven, 20 August - 16 September 2012., Berichte, MARUM - Zentrum für Marine Umweltwissenschaften, Fachbereich Geowissenschaften, Universität Bremen, p. 170.

Sahling, H., Römer, M., Pape, T., Bergès, B., dos Santos Fereirra, C., Boelmann, J., Geprägs, P., Tomczyk, M., Nowald, N., Dimmler, W., Schroedter, L., Glockzin, M., Bohrmann, G. (2014) Gas emissions at the continental margin west of Svalbard: mapping, sampling, and quantification. Biogeosciences 11: 6029-6046.

Sarkar, S., Berndt, C., Minshull, T. A., Westbrook, G. K., Klaeschen, D., Masson, D. G., Chabert, A., and Thatcher, K. E. (2012) Seismic evidence for shallow gas-escape features associated with a retreating gas hydrate zone offshore west Svalbard, J. Geophys. Res.-Sol Ea, 117, B09102.

Sato, T., Okuno, J., Hinderer, J., MacMillan, D., Plag, H.P., Francis, O., Falk, R., Fukuda, Y. (2006) A geophysical interpretation of the secular displacement and gravity rates observed at Ny-

Ålesund, Svalbard in the Arctic—effects of post-glacial rebound and present-day ice melting. Geophysical Journal International 165: 729-743.

Schmitt, M., Faber, E,. Botz, R., Stoffers, P. (1991) Extraction of methane from seawater using ultrasonic vacuum degassing. Analytical Chemistry 63: 529-532

Ślubowska-Wodengen, M., Rasmussen, T.L., Koç, N., Klitgaard-Kristensen, D., Nilsen, F., Solheim, A. (2007) Advection of Atlantic Water to the western and northern Svalbard shelf since 17,500 cal yr BP Quaternary Science Reviews 26: 463-478.

Svendsen, J.I., Alexanderson, H., Astakhov, V.I., Demidov, I., Dowdeswell, J.A., Funder, S., Gataullin, V., Henriksen, M., Hjort, C., Houmark-Nielsen, M., Hubberten, H.W., Ingólfsson, Ó., Jakobsson, M., Kjær, K.H., Larsen, E., Lokrantz, H., Lunkka, J.P., Lysså, A., Mangerud, J., Matiouchkov, A., Murray, A., Möller, P., Niessen, F., Nikolskaya, O., Polyak, L., Saarnisto, M., Siegert, C., Siegert, M.J., Spielhagen, R.F., Stein, R. (2004) Late Quaternary ice sheet history of northern Eurasia. Quaternary Science Reviews 23: 1229-1271.

Vanneste, M., Guidard, S., and Mienert, J. (2005) Bottom-simulating reflections and geothermal gradients across the western Svalbard margin, Terra Nova, 17: 510–516.

Vogt, P.R., Crane, K., Sundvor, E., Max, M.D., Pfirman, S.L. (1994) Methane-generated(?) pockmarks on young, thickly sedimented oceanic crust in the Arctic: Vestnesa ridge, Fram strait. Geology 22: 255-258.

Westbrook, G.K., Thatcher, K.E., Rohling, E.J., Piotrowski, A.M., Pälike, H., Osborne, A.H., Nisbet, E.G., Minshull, T.A., Lanoiselle, M., James, R.H., Hühnerbach, V., Green, D., Fisher, R.E., Crocker, A.J., Chabert, A., Bolton, C., Beszczynska-Möller, A., Berndt, C., and Aquilina, A. (2009) Escape of methane gas from the seabed along the West Spitsbergen continental margin, Geophys Res Lett, 36: L15608, 5 p.

Winkelmann, D. and Stein, R. (2007) Triggering of the Hinlopen/Yermak Megaslide in relation to paleoceanography and climate history of the continental margin north of Spitsbergen. Geochemistry, Geophysics, Geosystems 8(6): Q06018.

Wong, G.S.K. and Zhu, S. (1995) Speed of sound in seawater as a function of salinity, temperature and pressure. J. Acoust. Soc. Am. 97(3): 1732-1736.

9 Appendix

9.1 Station List

Heincke HE450 Station List

					Time (UTC)			on seafloor			
Date	StationNo	Instrument	GeoB	Location	on seafloor			Latitude	Longitude	Water	Recovery
2015	HE450	No.	St. No.		Begin	start	on deck	N	E	depth (m)	Remarks
27.08.2015	01-1	CTD-1	20201-1	SW-margin of Bjørnøya	06:00	06:12	06:36	74° 10.092'	16° 25.212'	353	-
27.08.2015	02-1	CTD-2	20202-1	SW-margin of Bjørnøya	07:19	07:35	08:04	74° 11.172'	16° 07.530'	691	-
27.08.2015	03-1	CTD-3	20203-1	SW-margin of Bjørnøya	14:42	14:55	15:10	74° 27.750'	16° 30.252'	256	-
28.08.2015	04-1	CTD-4	20204-1	Kveithola Trough Mouth	06:51	06:59	07:17	74° 49.812'	15° 54.540'	360	-
28.08.2015	05-1	CTD-5	20205-1	Kveithola Trough Mouth	08:00	08:08	08:24	74° 49.110'	15° 47.838'	361	-
28.08.2015	06-1	CTD-6	20206-1	Storfjorden southern TM	12:55	13:01	13:16	75° 17.748'	15° 01.820'	324	-
28.08.2015	07-1	CTD-7	20207-1	Storfjorden southern TM	14:30	14:38	14:55	75° 23.202'	14° 45.072'	374	-
29.08.2015	08-1	CTD-8	20208-1	North of Hornsund	12:26	12:31	12:38	76° 48.143'	14° 09.833'	103	-
29.08.2015	09-1	CTD-9	20209-1	North of Hornsund	14:22	14:29	14:43	76° 42.661'	13° 26.045'	244	-
30.08.2015	10-1	CTD-10	20210-1	Isfjorden northern TM	07:05	07:12	07:26	78° 16.348'	09° 49.996'	303	-
30.08.2015	11-1	CTD-11	20211-1	Isfjorden northern TMF	08:29	08:44	09:08	78° 17.251'	09° 17.916'	662	-
30.08.2015	12-1	BG-1	20212-1	Isfjordbanken Margin	-	13:40	13:49	77° 42.870'	10° 33.150'	405	few pebbles
31.08.2015	13-1	CTD-12	20213-1	Kongsfjorden	11:42	11:48	12:04	78° 57.520'	11° 55.043'	405	-
31.08.2015	14-1	MIC-1	20214-1	Kongsfjorden	12:36	12:49	-	78° 57.509'	11° 55.249'	356	-
31.08.2015	14-2	GC-1	20214-2	Kongsfjorden	13:26	14:04	-	78° 57.503'	11° 55.181'	356	3,5 m recovery
01.09.2015	15-1	CTD-13	20215-1	Kongsfjord Mouth	10:31	10:38	10:52	79° 01.347'	10° 46.248'	329	-
01.09.2015	16-1	CTD-14	20216-1	Forlandsundet Trough	11:49	11:55	12:05	78° 54.664'	11° 09.504'	214	-
01.09.2015	17-1	CTD-15	20217-1	Kongsfjord TMF	14:19	14:25	14:35	78° 55.523'	09° 35.768'	208	-
01.09.2015	18-1	CTD-16	20218-1	Kongsfjord TMF	15:45	15:50	16:01	78° 51.736'	08° 51.171'	221	-
02.09.2015	19-1	BG-2	20219-1	Isfjordbanken Margin	06:07	06:15	06:21	77° 42.834'	10° 33.704'	394	-
02.09.2015	20-1	BG-3	20220-1	Isfjordbanken Margin	06:33	06:43	06:49	77° 42.797'	10° 33.972'	392	-
02.09.2015	20-2	BG-4	20220-2	Isfjordbanken Margin	-	07:09	07:16	77° 42.786'	10° 34.087'	392	failure, w inch tangled
02.09.2015	20-3	BG-5	20220-3	Isfjordbanken Margin	-	07:28	-	77° 42.780'	10° 34.090'	392	-
02.09.2015	20-4	GC-2	20220-4	Isfjordbanken Margin	07:51	08:07	08:20	77° 42.786'	10° 34.087'	395	1,95 m recovery
02.09.2015	21-1	CTD-17	20221-1	Isfjordbanken Margin	09:15	09:23	09:37	77° 42.693'	10° 36.250'	349	-
02.09.2015	22-1	MIC-2	20222-1	Isfjordbanken Margin	10:07	10:24	-	77° 42.793'	10° 34.022'	393	5 cm hard stuff in one out of four tubes
02.09.2015	23-1	CTD-18	20223-1	Isfjordbanken Margin	12:52	12:55	13:01	77° 45.956'	12° 01.157'	87	-
02.09.2015	24-1	CTD-19	20224-1	Isfjordbanken Margin	15:53	16:00	16:10	78° 05.291'	10° 34.720'	219	-
03.09.2015	25-1	CTD-20	20225-1	Bellsundbanken Margin	07:31	07:42	08:04	77° 25.646'	11° 13.582'	519	-
03.09.2015	26-1	CTD-21	20226-1	Bellsundbanken Margin	09:06	09:12	09:22	77° 24.930'	11° 37.730'	195	-
03.09.2015	27-1	CTD-22	20227-1	Bellsundbanken Margin	12:37	12:45	12:55	77° 23.982'	12° 40.757'	244	-
03.09.2015	28-1	CTD-23	20228-1	Bellsundbanken Margin	14:21	14:25	14:32	77° 22.025'	13° 39.670'	77	-
04.09.2015	29-1	CTD-24	20229-1	Sørkappbanken	07:37	07:42	07:51	76° 30.738'	15° 00.958'	173	-
04.09.2015	30-1	CTD-25	20230-1	Sørkappbanken	10:51	10:20	10:26	76° 21.411'	16° 32.161'	48	-
04.09.2015	31-1	CTD-26	20231-1	Sørkappbanken	11:42	11:53	12:06	76° 12.348'	16° 02.358'	289	-
04.09.2015	32-1	CTD-27	20232-1	Sørkappbanken	13:43	13:51	14:06	76° 12.893'	15° 08.485'	340	-
05.09.2015	33-1	CTD-28	20233-1	Storfjorden southern TM	06:56	07:04	07:16	75° 26.584'	16° 26.177'	192	-
05.09.2015	34-1	CTD-29	20234-1	North of Kveithola	10:32	10:29	10:51	74° 57.471'	16° 54.541'	203	-
05.09.2015	35-1	CTD-30	20235-1	Kveithola	12:33	12:43	13:00	74° 48.649'	17° 39.498'	296	-
05.09.2015	36-1	CTD-31	20236-1	Kveithola	14:26	14:29	14:43	74° 49.122'	16° 53.242'	287	-
06.09.2015	37-1	CTD-32	20237-1	Northern Barents Sea Fan	05:58	06:04	06:15	74° 07.728'	17° 04.784'	213	-
06.09.2015	38-1	CTD-33	20238-1	Northern Barents Sea Fan	07:21	07:26	07:37	74° 04.890'	17° 41.583'	200	-
06.09.2015	39-1	CTD-34	20239-1	Northern Barents Sea Fan	12:04	12:15	12:34	73° 26.100'	18° 08.543'	447	-
06.09.2015	40-1	CTD-35	20240-1	Northern Barents Sea Fan	15:42	15:52	16:10	73° 29.460'	16° 20.661'	454	-
07.09.2015	41-1	CTD-36	20241-1	Southern Barents Shelf	10:46	10:51	11:01	71° 01.583'	18° 19.756'	196	-
07.09.2015	42-1	CTD-37	20242-1	Southern Barents Shelf	13:09	13:18	13:26	70° 52.161'	18° 49.930'	190	-

CTD CTD-Rosette
MUC Multicorer
UWMS Underw ater mass spectrometer
ISP In situ pumps
BG Grab sampler
SVP Sound velocity probe
GC Gravity corer

9.2 Sediment Cores

GeoB-Nr.:	**20212-1**
Station:	BG-1
Sample Type:	Grab Sample (Backengreifer)
Author:	Markus Loher

Purpose of this sampling:
This site was chosen in order to investigate the seafloor at a gas bubble emission site prior to taking a gravity core.

General description:
The grab sample is a poorly sorted, grain supported gravelly sand with a silty-clay matrix.
Neither the matrix nor any of the sand or gravel particles showed a reaction with 10% HCl.

Matrix:
dark greenish gray (Munsell colour 3/10Y) silt with some sticky clay

Larger grains:
The abundant sand and gravel grains are of a rounded to sub-angular nature and are poorly sorted (from millimetric to pluri-centimetric size).
The grains show a wide range of lithologies, such as:

- mm to max. 4 cm grains of rounded dark/black silt-/claystones (abundant)
- mm to max. 1 cm grains of rounded, reddish shales
- pluri-millimetric grains of yellow (altered?), milky as well as clear Quartz
- 1 cm sized schists / banded gneiss
- 1 cm sized, platy, brownish schists
- pluri-centimetric, friable clasts of mud containing different sedimentary grains (slight cementation)
- mm to max. 3 cm grains of rough, angular clasts, some encrusted by sponges

Biogenic components:

- Broken shell fragments (only few)
- Brittle Bryozoan / sponge (?) fragments
- Encrusting sponge material (on several pebbles)
- 1 cm long rods, cemented / agglutinated by sandy sediment grains
- 2-3 cm sized sea stars

Sediment Cores continued

GeoB-Nr.:	**20214-1**
Station:	MIC-1
Sample Type:	Mini-corer
Author:	Markus Loher

Purpose of this sampling:
First mini-corer deployment of the cruise, in the Kongsfjorden.
Sediment recovered: 11.5 cm

General description:
Brownish red clayey silt.

Matrix:
Brownish red, clayey silt.

Sediment Cores continued

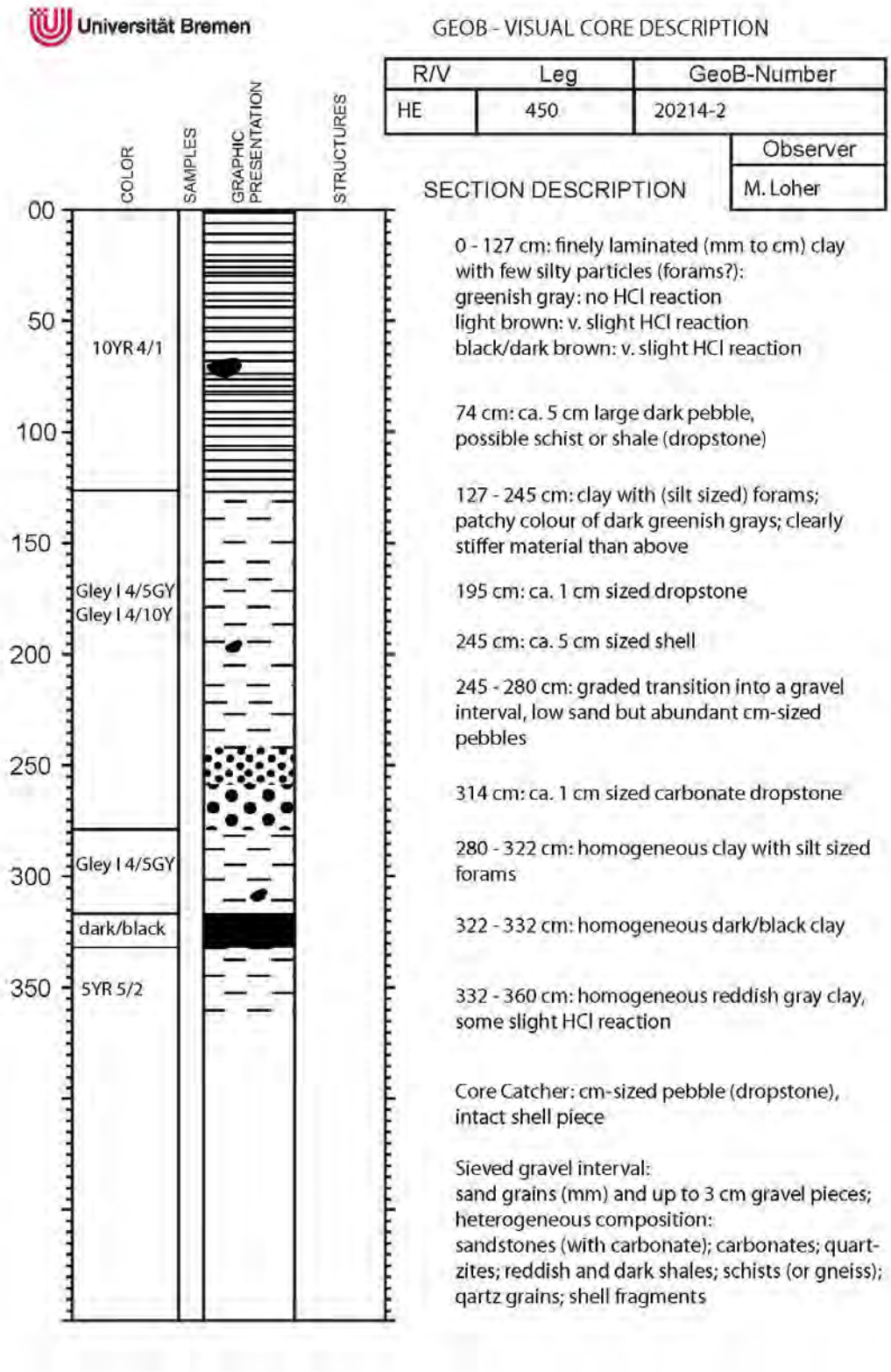

Sediment Cores continued

GeoB-Nr.:	**20219-1**
Station:	BG-2
Sample Type:	Grab Sample (“Backengreifer”)
Author:	Markus Loher

Purpose of this sampling:
This site was chosen in order to investigate the seafloor at a gas bubble emission site prior to taking a gravity core.

General description:
Poorly sorted gravelly sand with a silty matrix.

Matrix:
The fine grained sediment consists of silty material with some clay.

Larger grains:
The grains are of a heterogeneous nature ranging from mm (sandy) to pluri-cm.
Rounding ranges from well rounded to sub-angular.

- 8 cm clast of a strongly weathered, rounded, dark (reddish) brown rock, possibly sandstone
- 6 cm clast of a dark massive sandstone / shale
- 3 cm pebble of quartz
- 3 cm, angular sandstone clast
- 1 cm quartzite
- Up to 1 cm sized sand and pebbles: slightly more angular grains

Biogenic components:

- Brittle stars
- Sponges (?) encrusting some of the larger gravels

Sediment Cores continued

GeoB-Nr.:	**20220-1**
Station:	BG-3
Sample Type:	Grab Sample (“Backengreifer”)
Author:	Markus Loher

Purpose of this sampling:
This site was chosen in order to investigate the seafloor at a gas bubble emission site prior to taking a gravity core.

General description:
Poorly sorted, sandy gravel (possibly covering the immediate seafloor) with predominantly silty material as a matrix / down below.
Matrix:
Dark greenish gray (Munsell colour 3/10Y) silt with some sticky clay

Larger grains:
The larger components of this sample seem to be more abundant compared to the other samples of this site.

- over 10 cm diameter, weathered magmatic rock (granitic)
- a range of pebbles from 5 to 8 cm diameter (flat piece of sandstone, a more rounded light gray sandstone or quartzite
- pebbles of up to 1 cm: reddish shale, yellowish and white Quartz grains, dark shale or sandstone pieces
- carbonates seem rare

Biogenic components:

- Brittle stars
- Bryozoans
- Forams (sessile and benthic)
- Clam shell and remains (not gas-seep related; Astarte)
- Gastropods (“Napfschnecke”; Natica “Raubschnecke”)
- Sea urchins
- Sponges
- Polychetes (Sepula)

Sediment Cores continued

GeoB-Nr.:	**20220-3**
Station:	BG-5
Sample Type:	Grab Sample (“Backengreifer”)
Author:	Markus Loher

Purpose of this sampling:
This site was chosen in order to investigate the seafloor at a gas bubble emission site prior to taking a gravity core.

General description:
Poorly sorted, sandy gravel with a silty to sandy matrix.

Matrix:
Silty with sticky clay.

Larger grains:
A heterogeneous collection of pebbles and larger clasts includes:

- 16 x 13 x 8 cm sized, strongly weathered / altered rock (possibly sandstone), encrusted by sponges, carbonate tubes and strands of agglutinated sedimentary grains
- 7 cm diameter clast of a very porous, light grey sandstone with carbonate
- 5 x 8 cm, dark grey, massive sandstone
- Up to 7 x 10 cm, strongly weathered / altered rocks, possibly sandstone
- Up to 5 cm sized, dark shale
- 3 cm piece of coarse sandstone with some bedding
- 3 cm piece of altered/reddish quartzite
- Smaller grains (pluri-mm) composed from angular, dark shales, Quartz grains, sandstone,

Biogenic components:

- Shells
- Gastropods

Sediment Cores continued

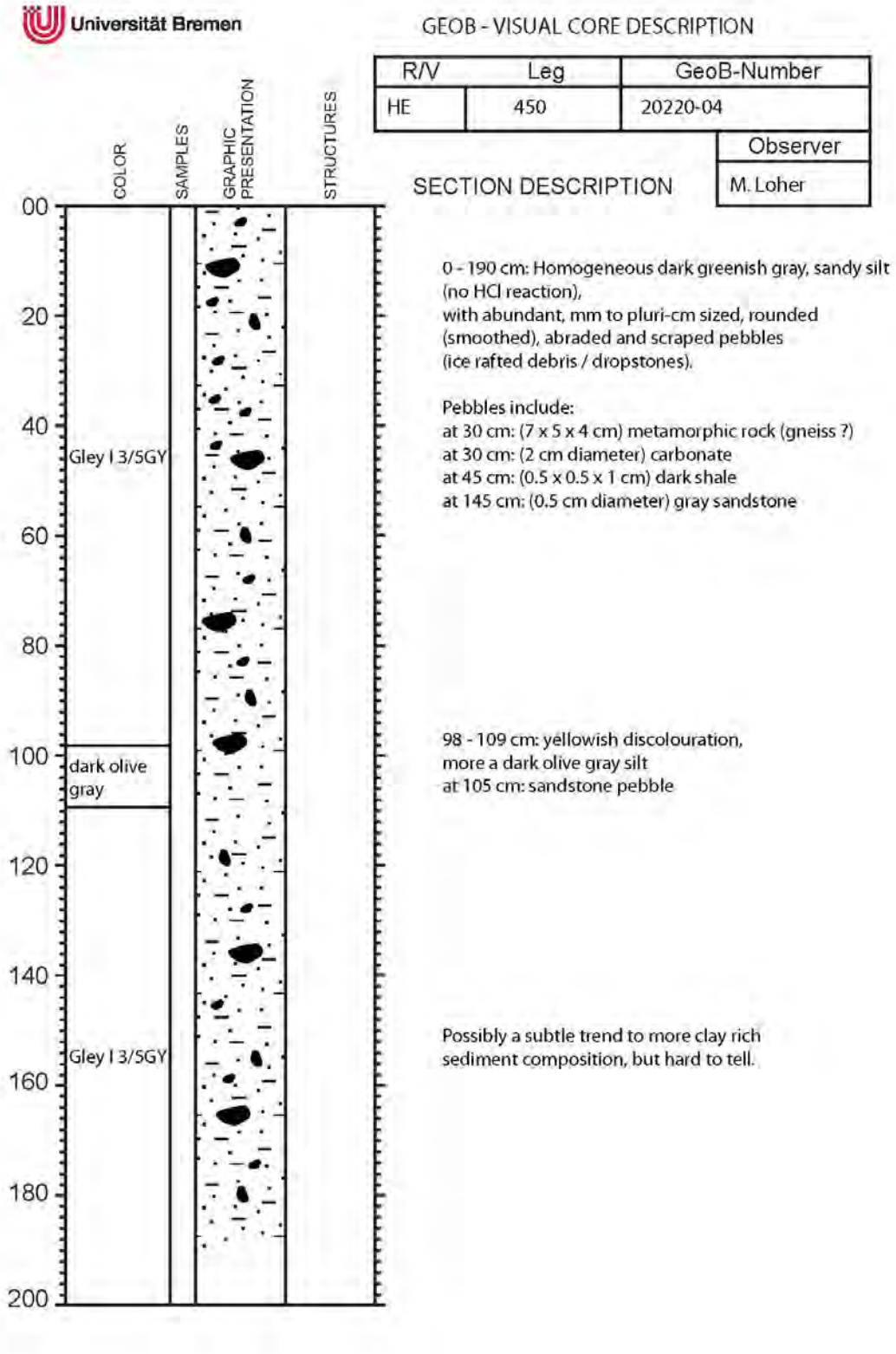

Sediment Cores continued

GeoB-Nr.:	**20222-1**
Station:	MIC-2
Sample Type:	Mini-corer
Author:	Markus Loher

Purpose of this sampling:
Only very little (ca. 5 cm) of sediment was retrieved in one of the MIC liners. The particles were washed and collected.

General description:
Silty sand with some coarser grains.

Matrix:
A homogeneous mud of silty clay.

Larger grains:

- 5 x 4 cm, very porous pieces of cemented mud/silt, strongly burrowed
- 2 cm, rounded piece of dark brown / altered pebble (sandstone?)
- Quartz grains (mm sized)
- Mm-sized grains cemented with mud
- Some pieces of dark/black schist or sandstone (hard to distinguish)